University
Printing

THE UNIVERSITY OF ALBERTA

THE HOOGENBOOM GAMMA RAY SPECTROMETER

A THESIS

SUBMITTED TO THE FACULTY OF GRADUATE STUDIES

IN PARTIAL FULFILMENT OF THE REQUIREMENTS FOR THE DEGREE

OF MASTER OF SCIENCE

DEPARTMENT OF PHYSICS

by

Walter Krawciw

Edmonton, Alberta

September, 1960

ACKNOWLEDGMENTS

I am very grateful for the assistance and cooperation of the following people who have made this project possible.

I should like to thank Dr. J. T. Sample, my supervisor and Drs. C. G. Neilson and W. K. Dawson for suggesting this project and for their willing guidance and assistance throughout the course of this program.

Thanks are also due to J. B. Elliott, L. Holm and C. F. Green for their technical help during the course of building and operating the equipment, and J. Easton for programing and calculations. Finally, I should like to thank Mrs. J. T. Sample for proofreading and Miss G. Tratt for typing the thesis.

TABLE OF CONTENTS

FIGURES

I. INTRODUCTION

Measurement of the energy emitted by an excited nucleus as it returns to the ground state is one of the principal methods of determining its energy level scheme. Below levels for which particle emission is energetically possible, the nucleus deexcites by emission of gamma rays of energy $h\nu$, h being the Planck constant, and ν the frequency of radiation. Thus a quantum of energy $h\nu$ corresponds to the energy difference between two levels in the nucleus. On emission of a gamma ray the nucleus suffers a recoil; the observed gamma ray energy, therefore, has a Doppler shift. This shift, however, is usually several orders of magnitude smaller than the actual energy and thus a correction to the measured value is not necessary. As an example of this there is a shift of 81 ev for a 1.28 Mev gamma emitted from Na^{22}.

Almost all methods used to detect gamma rays and measure their energies involve analysis of the secondary electrons produced when the gamma radiation passes through matter. The secondary electrons are produced by three processes: Compton scattering, photoelectric effect, and pair production. Thus a beam of gamma rays

of intensity I_o passing through material of thickness x will be reduced in intensity to I(x) where $I(x) = I_o \exp(-\mu x)$ and μ is the total absorption coefficient. The absorbed radiation produces secondary electrons. Since the three processes act incoherently the total absorption coefficient μ can be separated into three parts such that $\mu = \sigma + \tau + \kappa$ where σ is the absorption coefficient due to Compton scattering, τ due to photoelectric effect, and κ due to pair production.

The Compton interaction is the scattering of radiation from free electrons, the scattered radiation experiencing a shift toward longer wavelengths depending on the scattering angle θ. Using the principles of conservation of energy and momentum, it is easily shown (Ri)* that the amount of wavelength shift $\Delta\lambda$ is given by $\Delta\lambda = h/mc(1-\cos\theta)$ where h is the Planck constant, m the mass of the electron and c the speed of light. The Compton scattering cross section is given by the Klein-Nishima formula (He) which is derived by considering the interaction of the electromagnetic field of a gamma ray or photon with the electron. Using the relativistic

---

*References, indicated by the first two or three letters of the author's name, are listed on the last page of the thesis.

treatment of the electron, the differential scattering cross section per electron is found to be given by $d\sigma_e$ where

$$d\sigma_e = \frac{r_0}{2}\left\{\frac{1}{1+\alpha(1-\cos\theta)^2} \times \left[1+\cos^2\theta + \frac{\alpha^2(1-\cos\theta)^2}{1+\alpha(1-\cos\theta)}\right]\right\}$$

and

$$r_0 = e^2/mc^2 \quad , \quad \alpha = h\nu/mc^2$$

where e is the charge of an electron and ν the frequency of the incident gamma radiation. By integrating over the solid angle the total Compton cross section per electron becomes

$$\sigma_e = \pi r_0^2\left[\frac{1}{\alpha^3}\ln(1+2\alpha) + \frac{2(1+\alpha)(2\alpha^2-2\alpha-1)}{\alpha^3(1+2\alpha)^2} + \frac{8\alpha^2}{3(1+2\alpha)}\right]$$

Investigation of gamma scattering has shown (Se) that the Compton scattering is dominant in the energy range of 0.5 Mev to 5 Mev in lead and 0.05 to 15 Mev in aluminum. Since the scattering process is due to electrons the Compton cross section per atom is, therefore, proportional to Z, the atomic number of the scatterer.

In the photoelectric effect all the energy $h\nu$ of the gamma ray is transferred to a bound electron of an

atom which is then emitted from the atom with kinetic energy $T_e = h\nu - I$, where I is the binding energy of the electron, the excess momentum being taken up by the recoiling nucleus. Considering a hydrogen atom of charge Ze with one electron Heitler (He) calculates the photoelectric cross section τ_K thus:

$$\tau_K = \frac{8\pi r_0^2}{3} \frac{Z^5}{137^4} \left(\frac{mc^2}{k}\right)^{7/2} 2\sqrt{2}, \quad h\nu \gg I$$

and where $k = 2\pi/\lambda$ is the propagation vector of the gamma ray with energy $h\nu$ and r_0 is as previously defined. The photoelectric effect is found to be the principal interaction below 50 Kev for aluminum and 500 Kev for lead.

For gamma rays with energies of 1.02 Mev or greater the third process, pair production, may occur. In this process 1.02 Mev of the gamma energy is used to produce an electron-positron pair; the excess energy becomes the kinetic energy of the electron and positron. Pair production occurs only in the Coulomb field of a charged particle. The Coulomb field is necessary to give a non-zero matrix element for the transition (pair production by photon-photon interaction is extremely unlikely). The Coulomb field is usually supplied by a

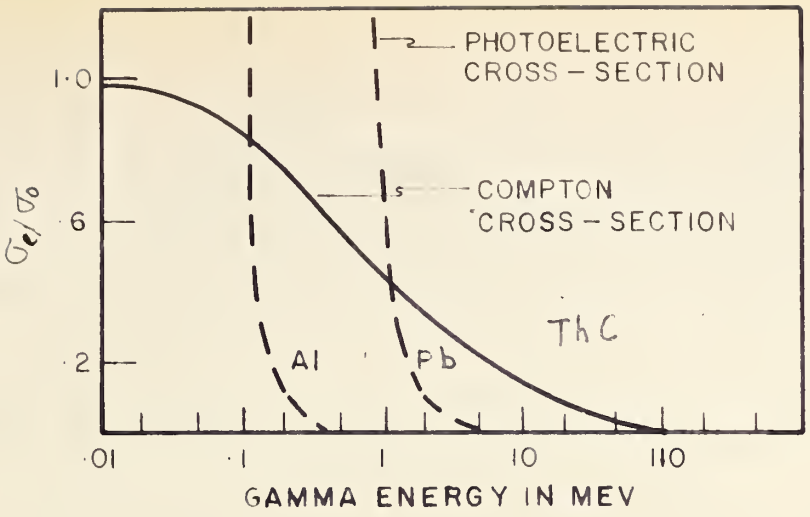

cross section in units of σ_0

$\sigma_0 = \frac{8\pi}{3} r_0^2$

FIG·1-1

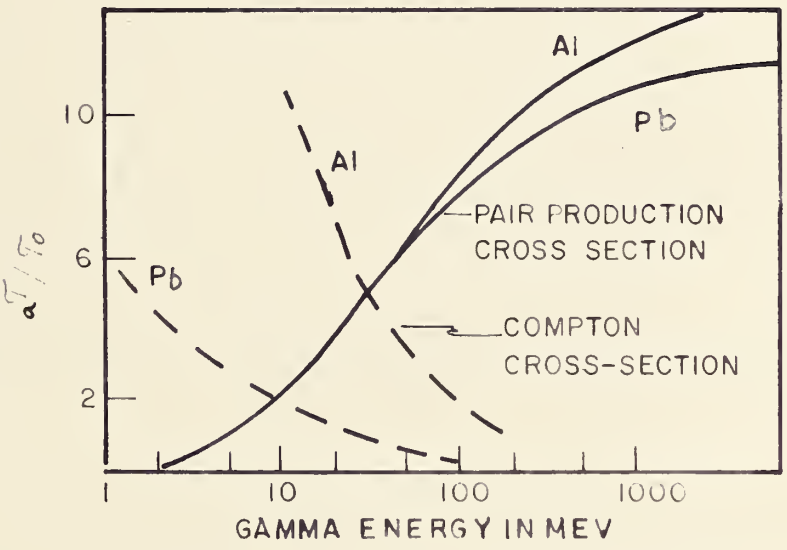

cross section in units of τ_0

$\tau_0 = \frac{Z^2}{137} r_0^2$

FIG·1-2

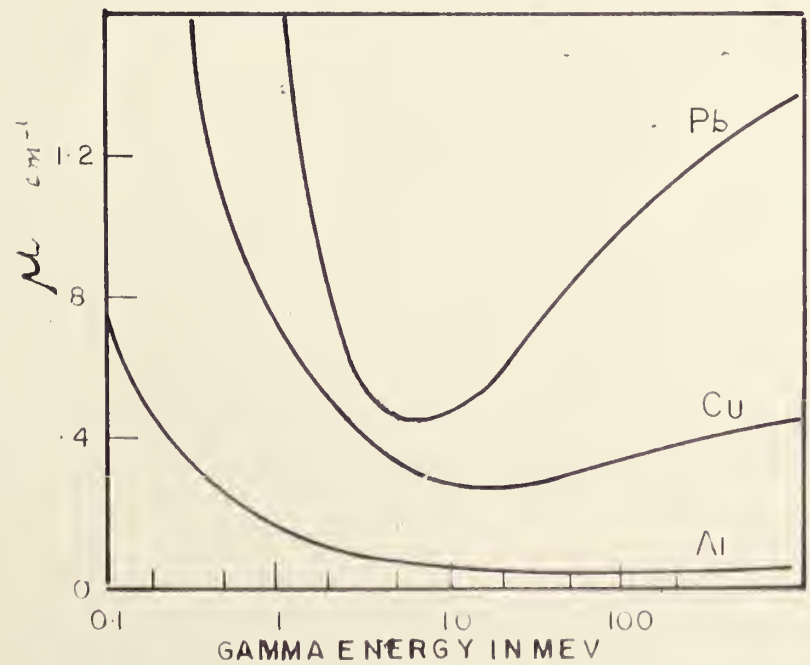

total absorption coefficient μ in units of cm^{-1}

FIG·1-3

nucleus; the electron field may also produce such a transition but the probability is much smaller. With the relativistic treatment of the electron, one finds the total pair formation cross section κ (He) to be given by

$$\kappa = \frac{Z^2}{137} r_0^2 \left(\frac{28}{9} \ln \frac{183}{Z^{1/3}} - \frac{2}{27}\right) \qquad \text{(complete screening)}$$

for high energy gamma rays; that is, $h\nu \gg mc^2$. For the lower energy case the expression is much more involved and cannot be completely integrated; the differential cross section for positron of energy between E_+ and $E_+ + dE_+$ and electron energy E_- for energy range $2 \leq h\nu/mc^2 \leq 15$

$$\kappa(E_+)\,dE_+ = \frac{4Z^2 r_0}{137} \frac{dE_+}{k^3} \left(E_+^2 + E_-^2 + \frac{2}{3} E_+ E_-\right)\left(\ln \frac{2E_+E_-}{h\nu mc^2} - \frac{1}{2} - C\alpha\right)$$

where r_0, k, α are as previously defined and $C(\alpha)$ is a complex function of energy shown in Segrè (Se 1). Soon after its formation, the positron annihilates an electron, producing, in most cases, two oppositely directed photons, each with 0.51 Mev energy. Pair production is found to be dominant above 5 Mev in lead and 15 Mev in aluminum.

The variation of individual cross sections σ, τ and κ and total cross sections μ as a function of

energy can be observed from graphs (Se) shown in Fig. 1-1 to 1/3. From Fig. 1-1 it is seen that the photoelectric cross section σ_a decreases very sharply with increasing gamma ray energy and is effectively zero at 0.25 Mev in aluminum and 7.5 Mev in lead. The Compton cross section σ_c decreases exponentially with an increase in energy and becomes negligible at about 500 Mev in lead. Pair production becomes effective for gamma rays with energies of 2.5 Mev or greater and steadily increases with an increase in gamma energy. It can be observed from Fig. 1-3 that the total absorption coefficient μ decreases sharply with increase in gamma energy going through a minimum, and then increases slowly at higher energies. The position of the minimum depends on the element, which occurs between 2.5 Mev and 5 Mev.

It is well known that the passage of charged particles through matter causes ionization. In some gases, liquids, plastics, and crystals light of a frequency to which the material is transparent is also emitted (Ka). The electrons produced by gamma ray interactions produce such flashes of light in these materials. The intensity of the emitted light is dependent on the amount of energy loss in the material, and this light, known as luminescence, can be increased in some materials by certain

impurities called activators. Crystalline sodium iodide containing less than 1% thallium, which has a high mean atomic number and high light output, is suitable for detecting gamma radiation.

The light output of a crystal is detected by a photomultiplier tube which produces a pulse of electric charge proportional in magnitude to the number of photons striking its photo-cathode. The scintillation counters have proven to be more efficient with much better energy resolution than proportional counters previously used to measure gamma ray energies. The resolution does not, however, approach that of magnetic spectrometers but the scintillation spectrometer is much more efficient and compact.

Because the scintillator responds to electrons which are due to the three types of gamma interactions, the resulting pulse height spectrum from a monoenergetic beam of gamma rays will be due to all the possible interactions. A gamma ray with energy below that required for pair formation may lose its energy to the crystal by Compton interaction or by photoelectric effect. In the Compton interaction, only part of the primary photon energy becomes kinetic energy of the electron and the remainder of the energy is carried by the secondary photon. The secondary photon may escape from the crystal

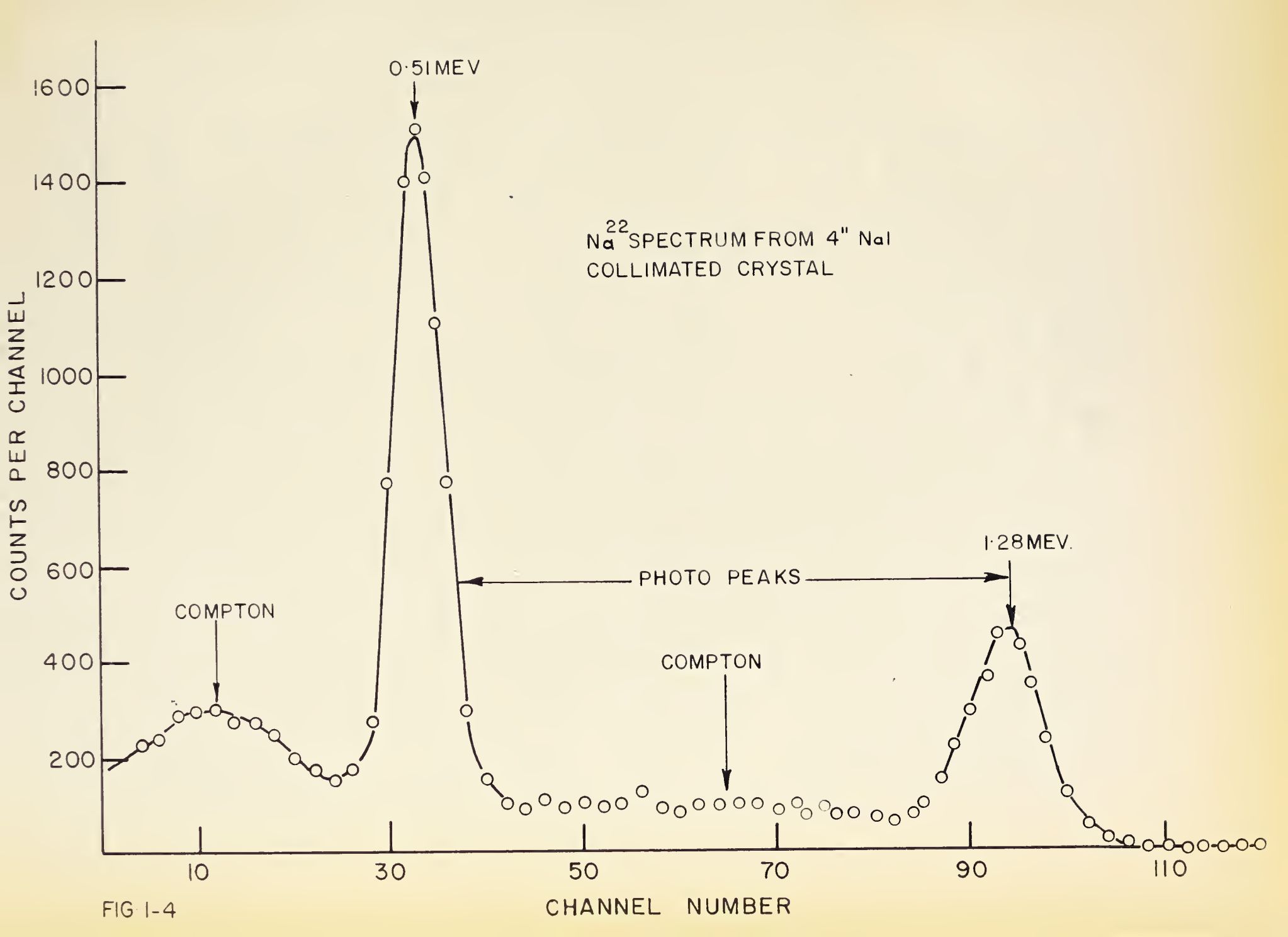
0·51MEV
1600
1400
1200
1000
800
600
400
200
COUNTS PER CHANNEL
Na22 SPECTRUM FROM 4" NaI
COLLIMATED CRYSTAL
1·28MEV.
PHOTO PEAKS
COMPTON
COMPTON
10
30
50
70
90
110
CHANNEL NUMBER

FIG 1-4

or release further electrons by Compton or photoelectric interactions and thus produce more light in the crystal. This secondary light adds to that produced by the primary electrons resulting, when no photons or electrons leave the crystal, in a light output which is proportional to the primary photon energy. The separate stages of interaction occur nearly simultaneously, so that their total light output results in a single pulse of charge from the photomultiplier. The pulse height distribution due to a beam of monoenergetic gamma rays as recorded by a pulse height analyzer consists of a peak preceded by a broad Compton distribution. The peak, which will be referred to as the "photo peak", is due to the complete absorption of the gamma ray either by photoelectric effect or by multiple scattering and the "Compton distribution" due to the absorption of only part of the gamma energy. Each photo peak will, therefore, have its Compton spectrum except in the case of very large crystals into which the gamma beam is collimated. Fig. 1-4 illustrates a spectrum of Na^{22} which shows two photo peaks 0.51 Mev and 1.28 Mev and the corresponding Compton spectra. The channel number scale corresponds to the relative pulse height of the spectrum.

A gamma energy of at least 2.5 Mev is required to form pairs in quantity comparable to Compton electrons

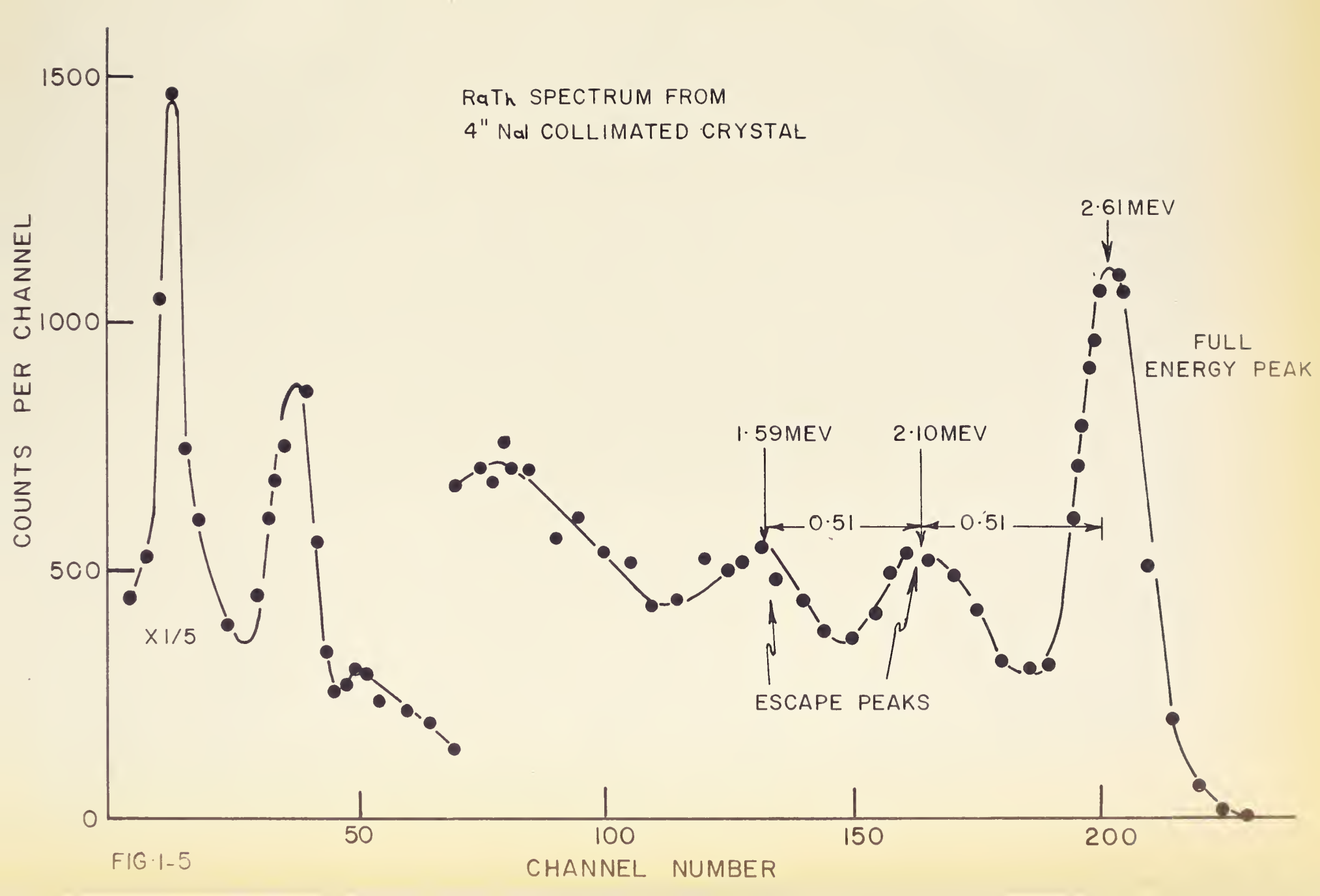
RaTh SPECTRUM FROM
4" NaI COLLIMATED CRYSTAL
COUNTS PER CHANNEL
1500
1000
500
0
X1/5
2·61MEV
FULL
ENERGY PEAK
1·59MEV
2·10MEV
0·51
0·51
ESCAPE PEAKS
50
100
150
200
CHANNEL NUMBER

FIG·1-5

since the pair cross section is very small above the threshold at 1.02 Mev. The spectrum from a beam of high energy gamma rays incident on a crystal is more complex than the one of lower energy as is illustrated by the spectrum of RaTh in Fig. 1-5. An energetic gamma photon may lose its energy with appreciable probability by pair formation though Compton scattering dominates below 30 Mev. The positron, produced in the interaction, annihilates with an electron after slowing nearly to rest, resulting in two gamma photons. Depending on the position in the crystal at which annihilation occurs, one or both gammas may escape. Thus, for a single high energy gamma ray three peaks result unless the gamma rays are collimated into a very large crystal to ensure the absorption of both annihilation gamma rays. The peak corresponding to the greatest energy captured by the crystal is due to pair formation, plus total absorption of both annihilation photons, the next peak down is due to pair formation and the absorption of only one annihilation photon and the lowest peak is due only to the kinetic energy of the pair. The energy difference between the adjacent peaks is 0.51 Mev. The fast electrons produced from very high gamma energy, 10 Mev or greater, produce bremstrahlung radiation which greatly reduces the

resolution of the photo peak. When the electrons are not completely stopped in the crystal the resolution of the photo peak is also highly reduced. Consequently, these effects make the crystal ineffective at high energies. A single crystal spectrum resulting from a beam of gamma rays with different energies is consequently very complicated and often impossible to analyze.

A further complication to the spectrum arises in the case where neutrons are present. I^{137} in a NaI crystal captures neutrons followed by prompt emission of gamma rays in the energy range of 4 to 6 Mev followed by 2 Mev beta decay (Sa). The effect of this neutron capture is to raise the background level and obscure the peaks corresponding to the gamma rays of interest.

An ideal spectrometer would be one which would produce only one peak in the pulse height spectrum for a gamma ray of a given energy, with good resolution and high efficiency. By sacrificing efficiency, spectrometers have been designed which identify each gamma energy with one peak of increased resolution. The two-crystal Compton spectrometer, the three-crystal pair spectrometer, the anticoincidence spectrometer, and the Hoogenboom spectrometer have all been developed for this purpose.

The two-crystal spectrometer developed by Hofstadter

COMPTON SPECTROMETER

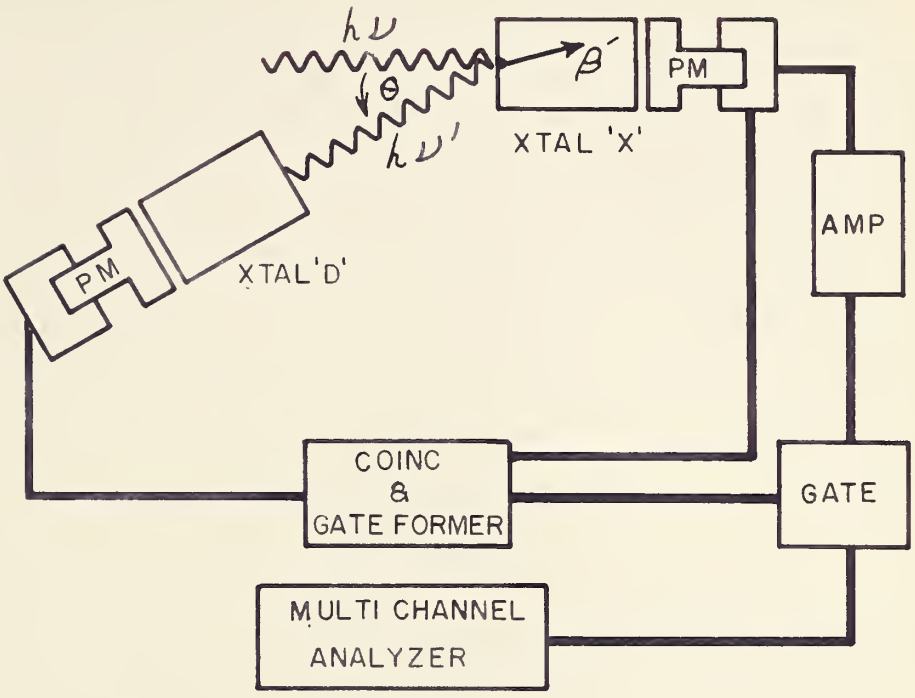

FIG. 1-6

THREE CRYSTAL SPECTROMETER

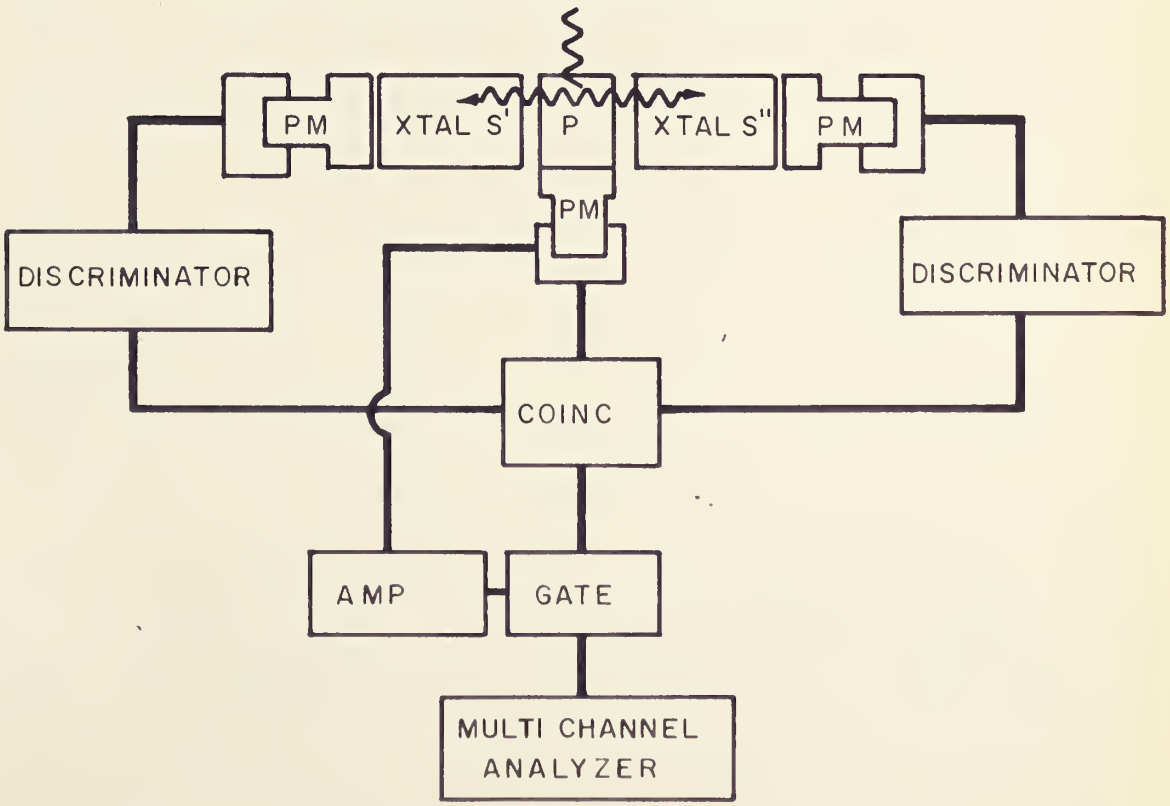

FIG. 1-7

and McIntyre (Ho) utilizes only the Compton scattering process. A beam of gamma rays of energy $h\nu$ incident on crystal X, shown in Fig. 1-6, is scattered at an angle θ into crystal D with the scattered electron β recoiling in crystal X. The scattered gamma $h\nu'$ loses its energy in crystal D by further Compton scattering or by photoelectric process, producing a flash of light in crystal D, while crystal X produces a signal due to electron β. The pulses from crystal D, being in coincidence with X, are used to gate the pulse size distribution from X. Consequently the displayed spectrum consists of a single peak for each energy. The position of crystal D is, however, limited to a particular angular range for best resolution, thus limiting the scattered gammas to a particular part of the Compton spectrum. At energies greater than 1.5 Mev additional lines have been observed which are due to pair formation. For several high energy gamma rays the spectrum will then be complicated by the pair lines and will become difficult to analyze. The pair effect, however, has been used to advantage in developing the three crystal spectrometer.

The three crystal spectrometer (Ma) consists of a primary crystal P and two secondary crystals S' and S", as shown in Fig. 1-7. A beam of collimated gamma rays with energies greater than 1.5 Mev are incident on

ANTI - COINCIDENCE SPECTROMETER

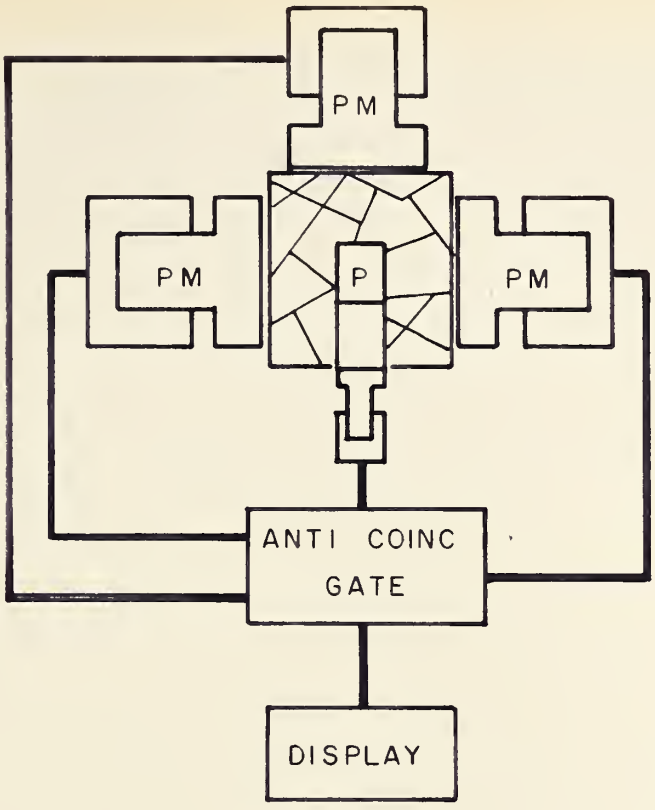

FIG. I-8

COINCIDENCE SPECTROMETER

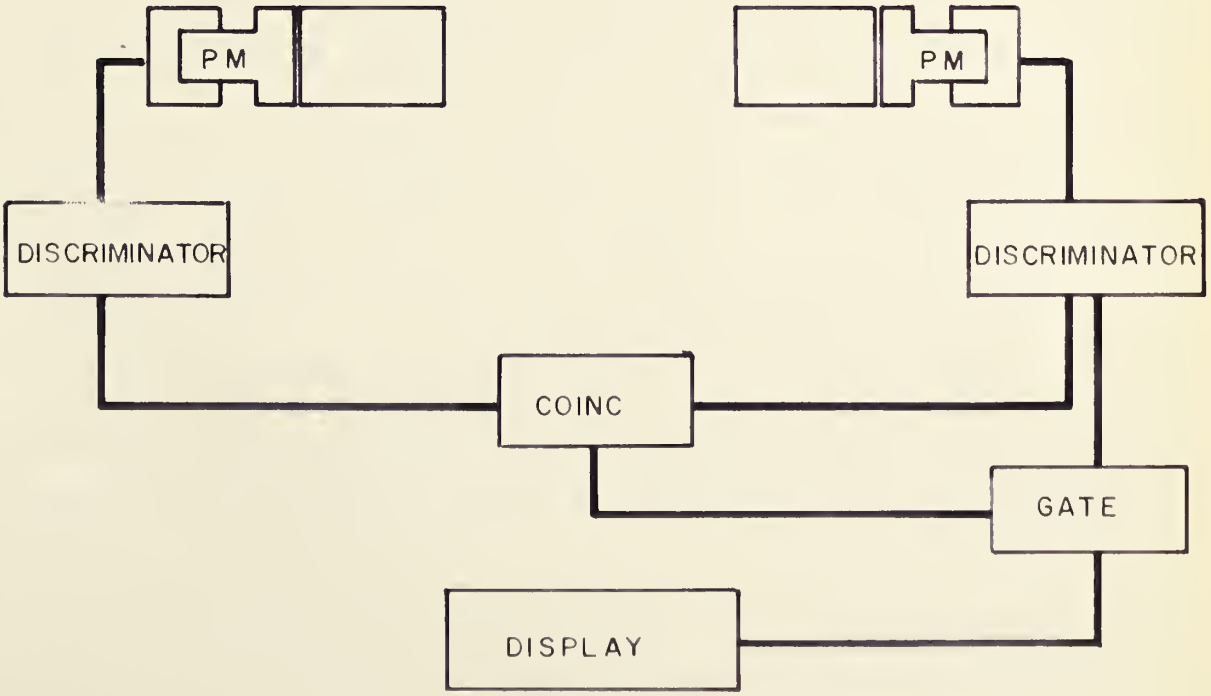

FIG. I - 9

the primary crystal. The gammas produce pairs with the annihilation photons being detected in S' and S" simultaneously, resulting in a triple coincidence. The coincidence output of S', S" and P is used to gate the energy spectrum from crystal P. This type of spectrometer has been used to measure gamma ray energies up to 10 Mev (Sa). At higher energies the spectrometer loses resolution as all the secondary electrons produced are not completely stopped in the primary crystal. A possible solution to this problem is to increase the physical size of the crystal. This, however, complicates the matter by introducing a higher background and noise level in the spectrometer, thus resulting in a small improvement, if any, over the smaller primary crystal.

After the development of the three-crystal spectrometer, a multi-crystal spectrometer was developed by Albert (Al) Fig. 1-8 which consisted of a primary crystal surrounded by a cluster of small secondary crystals. The cluster of crystals is used to detect photons scattered from the primary crystal arising from gamma rays which do not transfer their entire energy to the primary crystal. All the signals in the primary crystal resulting from gammas which are Compton scattered from the primary crystal into the secondaries are removed by an anti-coincidence circuit, as are the signals resulting from

pair formation in which both annihilation gamma rays are not absorbed. The resulting spectrum, therefore, consists of only the fully absorbed gamma rays.

The spectrometers described above are not easily used for angular correlation measurements, nor are they suited for identifying the cascading gamma rays from the complete spectrum of a highly excited nucleus. The two crystal coincidence spectrometer (Si) has been used to detect and measure the energy of the cascade gammas. The spectrometer (Fig. 1-9) consists of two crystals, two differential discriminators, a coincidence circuit and a gated display system. The spectra of a given gamma course from the two crystals are nearly identical and are composed of photo peaks and Compton distributions as have been described earlier.

To determine which of the gamma rays are the cascading gammas of a given gamma spectrum, the differential discriminator of one crystal is set on a particular photo peak to gate the gamma spectrum from the other crystal. The gated spectrum consists of only the gamma rays which are in coincidence with the gamma ray determined by the setting of the differential discriminator. These coincident gammas are the cascading gammas from some energy level of an excited nucleus. The energy level of the nucleus from which the gammas cascade

may be determined by eliminating some of the cascade gammas by using the second discriminator. For a well resolved spectrum the cascade gammas can be easily determined. However, for a complex spectrum the spectrometer is not so successful because of the single crystal complications described earlier. Recently a spectrometer has been built which is particularly designed for determining the cascade gammas from a complex spectrum.

The Hoogenboom spectrometer (Fig. 2-1), as it is called, was designed by Hoogenboom in 1958 (Hoo). This spectrometer, which is a development of the coincidence spectrometer, is used to identify cascade gamma rays and, at the same time, establish the energy level of a nucleus from which the gamma rays cascade. These quantities can be determined simultaneously due to the fact that the total energy in different cascades from a particular energy level is the same. This total energy is obtained by adding together the energies of the cascading gammas. Identical spectra of the cascade gamma rays are obtained from the two detecting NaI crystals, then are added in a linear adding circuit to form a sum spectrum. The sum spectrum includes a photo peak which corresponds to the total energy of the cascades as well as a distribution due to the non-cascading gammas and the various Compton distributions. A differential

discriminator set on the sum peak and a coincidence circuit between the two detectors are used to eliminate all the gammas except the ones which cascade from the given energy level. The adding circuit together with the differential discriminator are equivalent to the two differential discriminators used in the coincidence spectrometer. The discriminator setting on the sum spectrum determines the energy of the level from which the gamma rays cascade.

When the differential discriminator is set on the sum peak, all the gamma rays which do not transfer their energy to the crystal completely and all the non-cascading gammas are eliminated. The displayed spectrum, therefore, consists of only full energy peaks, removing all the Compton distributions normally observed in a single crystal spectrum. As will be shown in a later section, the absolute peak width (defined as the full width of the peak at half the maximum height)is the same for all the cascading gammas. This gives the Hoogenboom spectrometer an improved resolution for the same energy gammas in a cascade over the single crystal spectrometer and the previously outlined spectrometers. Because the half width remains constant to a first approximation, the improvement in resolution should be most evident for the high energy gamma rays. The theoretical derivation also indicates that the detection

HOOGENBOOM SPECTROMETER

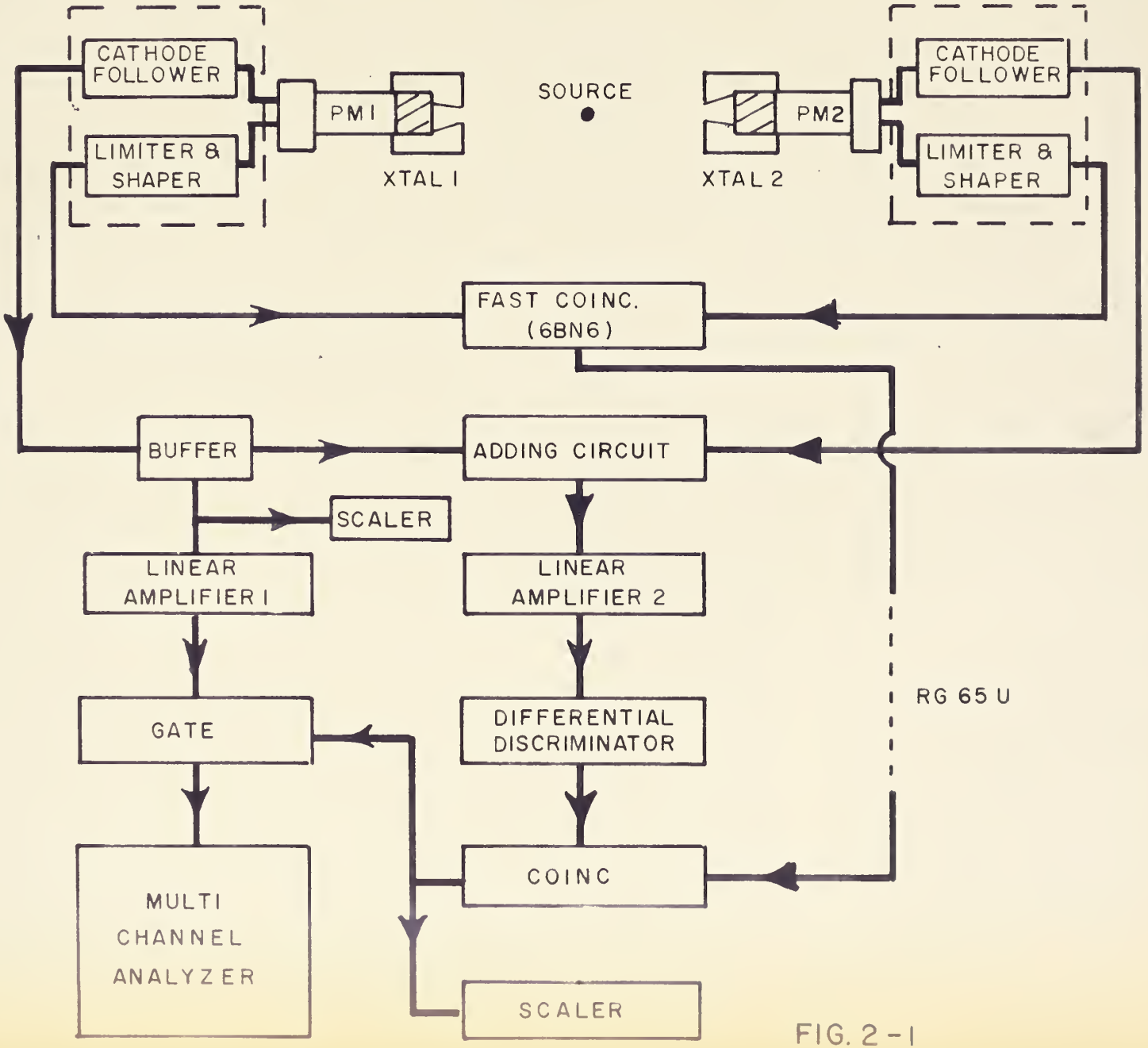

FIG. 2-1

efficiency of each coincident gamma ray is the same. As detection of each cascading gamma ray has equal probability the area under each full energy peak should be the same. All these Hoogenboom characteristics are dependent on the sum spectrum. It is, therefore, necessary to ensure that the two single crystal spectra are identical in size and shape, otherwise the Hoogenboom spectrum will not have these properties.

A Hoogenboom spectrometer has been built to analyze the cascade spectra resulting from bombardment of light elements with protons and deuterons. It has been tested by use of the cascading gammas from Na^{22} and Co^{60}.

II. APPARATUS

1. General

The complete Hoogenboom spectrometer is shown in schematic diagram 2-1. Two different sets of detectors have been used, one being 2" diameter x 2" long crystal mounted on RCA 6342 photomultipliers, the other 4" diameter x 4" long crystal on RCA 7046 photomultipliers, and each crystal is shielded with 2" of lead. Anode signals from the photomultipliers PM 1 and PM 2 are transmitted by cathode followers to the adding circuit. Dynode signals from PM 1 and PM 2 are shaped and transmitted to the fast coincidence circuit. The sum signal is amplified and then analyzed by a differential discriminator. The output of the discriminator is then checked for coincidence with the output of the fast circuit, coincident pulses being used to form a gating pulse which is counted by a scalar. The spectrum signal is taken from anode of PM 1 and transmitted by a cathode follower to a linear amplifier, the output of which is passed through a gate controlled by the coincidence output. The gated output is displayed on a multi-channel pulse height analyzer. For the signal to be gated through to the analyzer two conditions have to be satisfied:

1. The display signal from PM 1 must be in coincidence with a signal in PM 2.

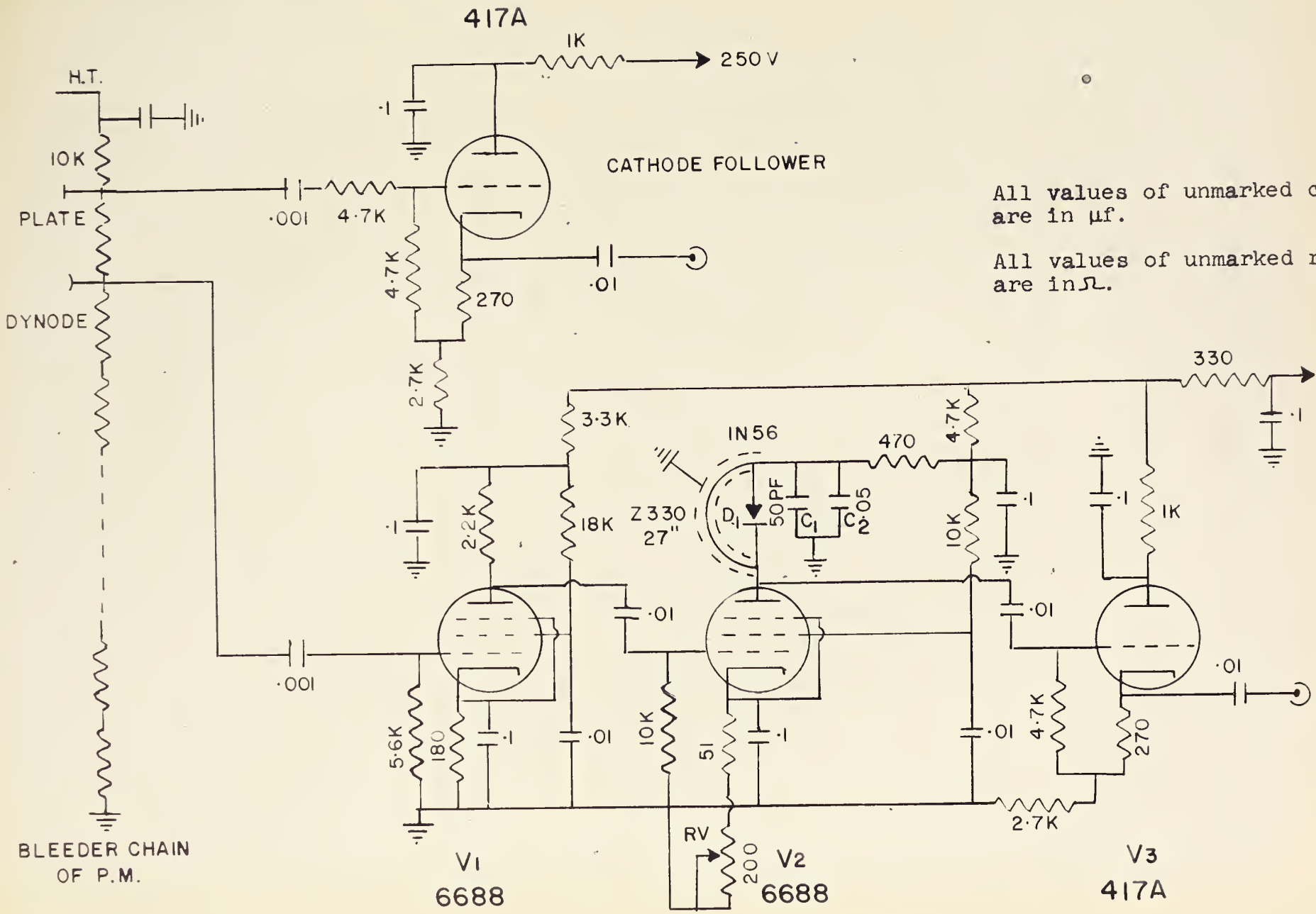

FIG· 2-2

LIMITER AND SHAPER

2. The pulse height from PM 2 must be of such a value that when added to the pulse height from PM 1 it forms a sum pulse whose peak voltage falls within the differential interval of the discriminator.

The circuitry is described in greater detail in the following sections.

2. Limiter and Shaper (Fig. 2-2)

The limiter and shaping circuit consists of an amplifier tube V1, a limiting tube V2, and a cathode follower tube V3. A positive signal from the photomultiplier is amplified by a factor of 10 in V1 and the amplified signal is then limited by cutting off V2, the gain of which may be adjusted by the potentiometer RV. The pulse shaping is completed by a shaping network consisting of Z330 transmission cable, capacitors C_1, C_2 and diode D_1. Pulse shaping by this network can be described as follows.

A square positive pulse appearing at the input of the transmission cable traverses the length of the cable in time TL where T is the time delay per unit length of the cable and L is the total length of the cable. If the other end of the cable is short circuited, the pulse is reflected 180° out of phase, cancelling the remainder of the pulse travelling in the forward direction. The remaining negative pulse is short circuited to ground by diode D_1 and capacitors C_1 and C_2, C_1 being the low

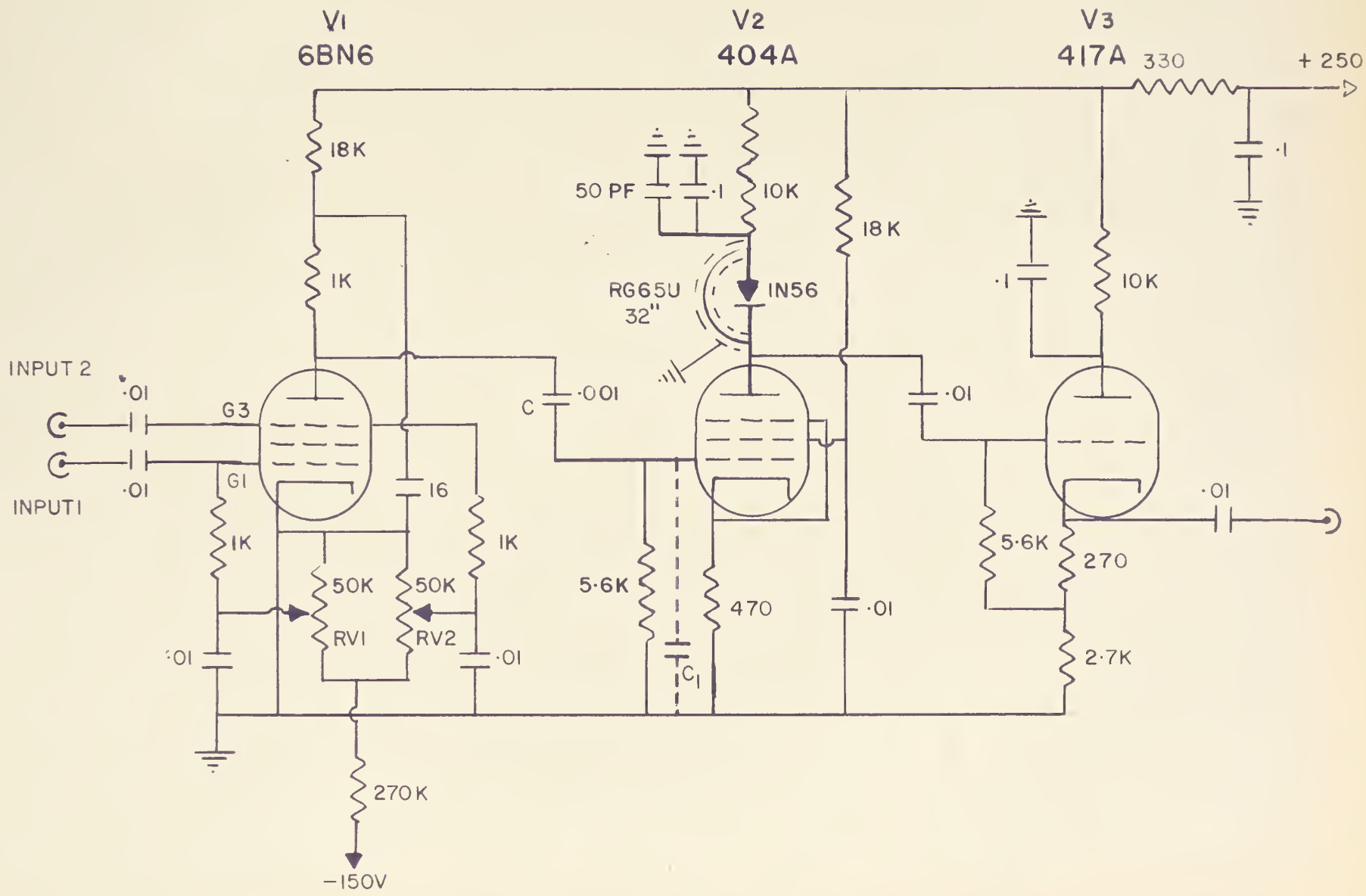

FIG. 2-3 FAST COINCIDENCE

minimum capacity signal are obtained at the plate of the 6BN6 when the signals overlap in time as shown in Fig. 2-4b. The capacity signal, the signal which appears at the plate of the tube due to grid plate capacitance, is present whether or not the input signals are coincident. A rejection ratio, that is the ratio of the amplitudes of the coincidence pulse to the amplitude of the capacity pulse, of 15 is obtained using 2.5 volt, 100 nanosecond rectangular input pulses. The condition for time coincidence of the input pulses requires that the time between corresponding points on the pulses be less than the resolving time of the coincident circuit. The resolving time t of this circuit is 2×10^{-7} sec.

The output signal from 6BN6 is integrated by the stray capacity C_1. Hence the voltage amplitude of this signal is proportional to the amount of time overlap of the tw input pulses thus transforming the time distribution to a pulse height distribution as shown in Fig. 2-5. It is possible to improve the resolving time of the circuit by a factor of 10 by setting a pulse height discriminator on the integrated pulse. By setting a discriminator on the peak of this distribution all the partially overlapped pulses are eliminated.

PULSE SHAPING

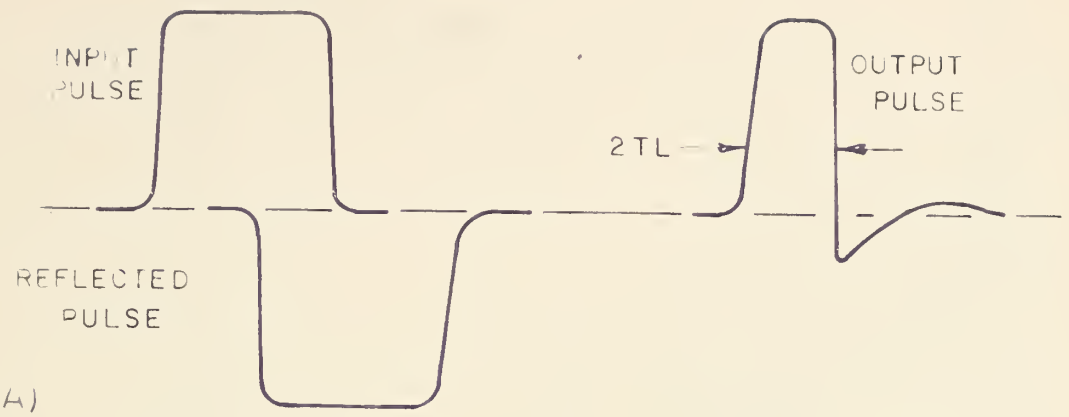

FIG. 2 - 4 (A)

COINCIDENCE OUTPUT

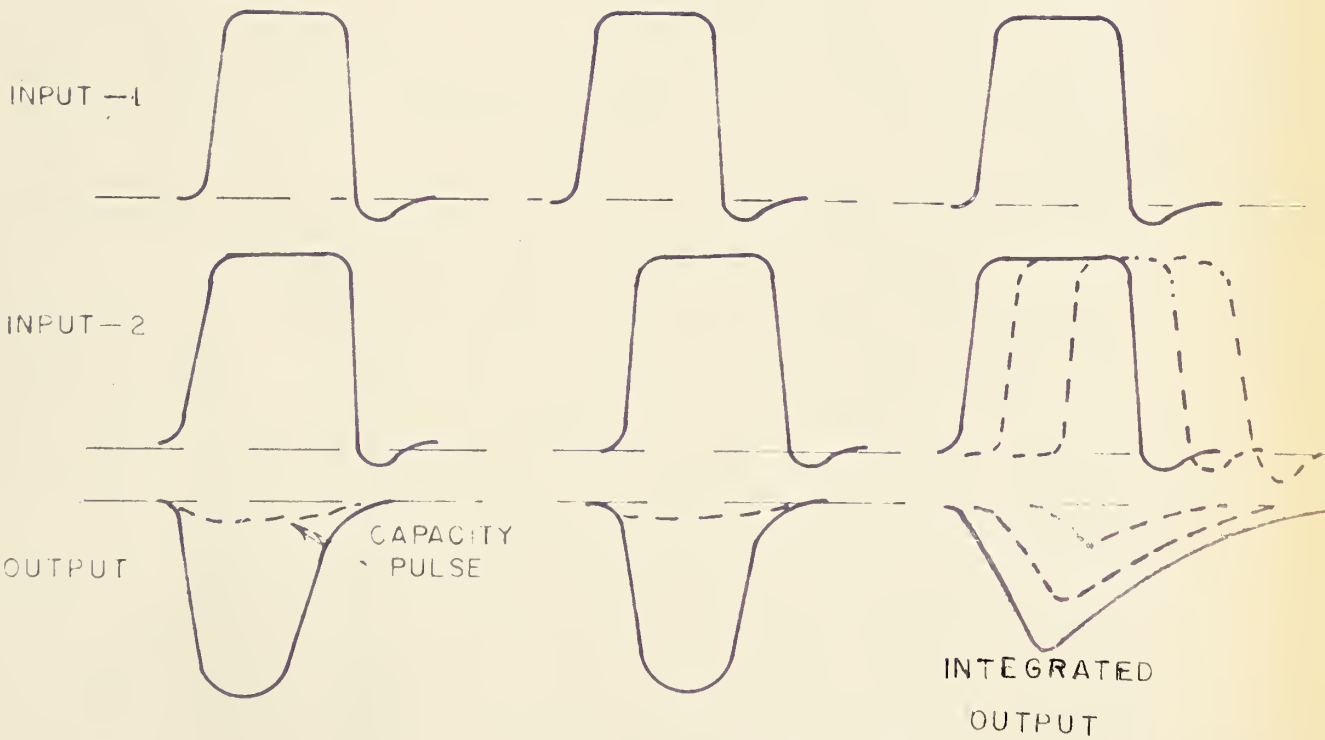

FIG. 2 - 4(B)

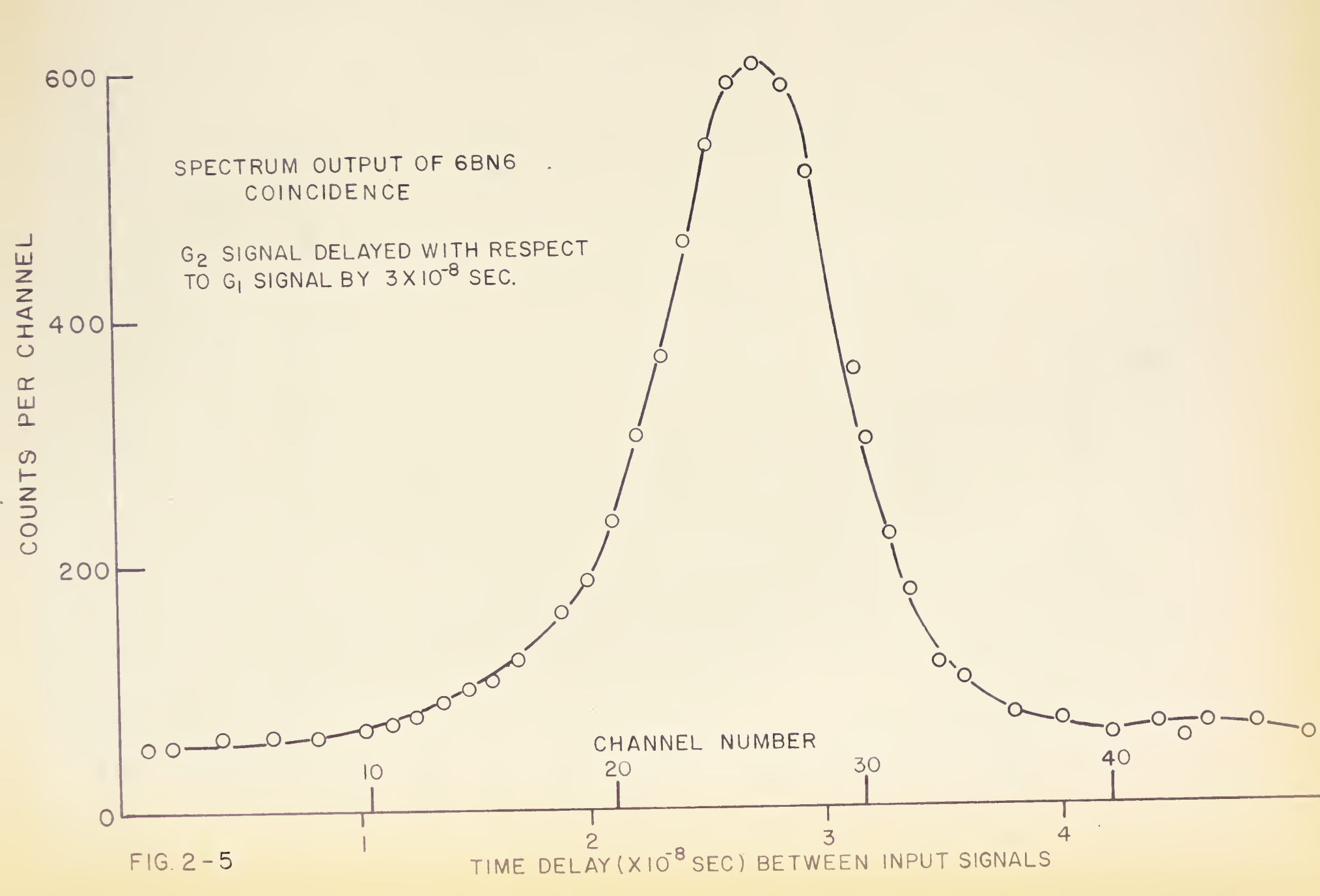
SPECTRUM OUTPUT OF 6BN6
COINCIDENCE
G_2 SIGNAL DELAYED WITH RESPECT
TO G_1 SIGNAL BY 3×10^{-8} SEC.
COUNTS PER CHANNEL
600
400
200
0
CHANNEL NUMBER
10
20
30
40
1
2
3
4
TIME DELAY ($\times 10^{-8}$ SEC) BETWEEN INPUT SIGNALS

FIG. 2-5

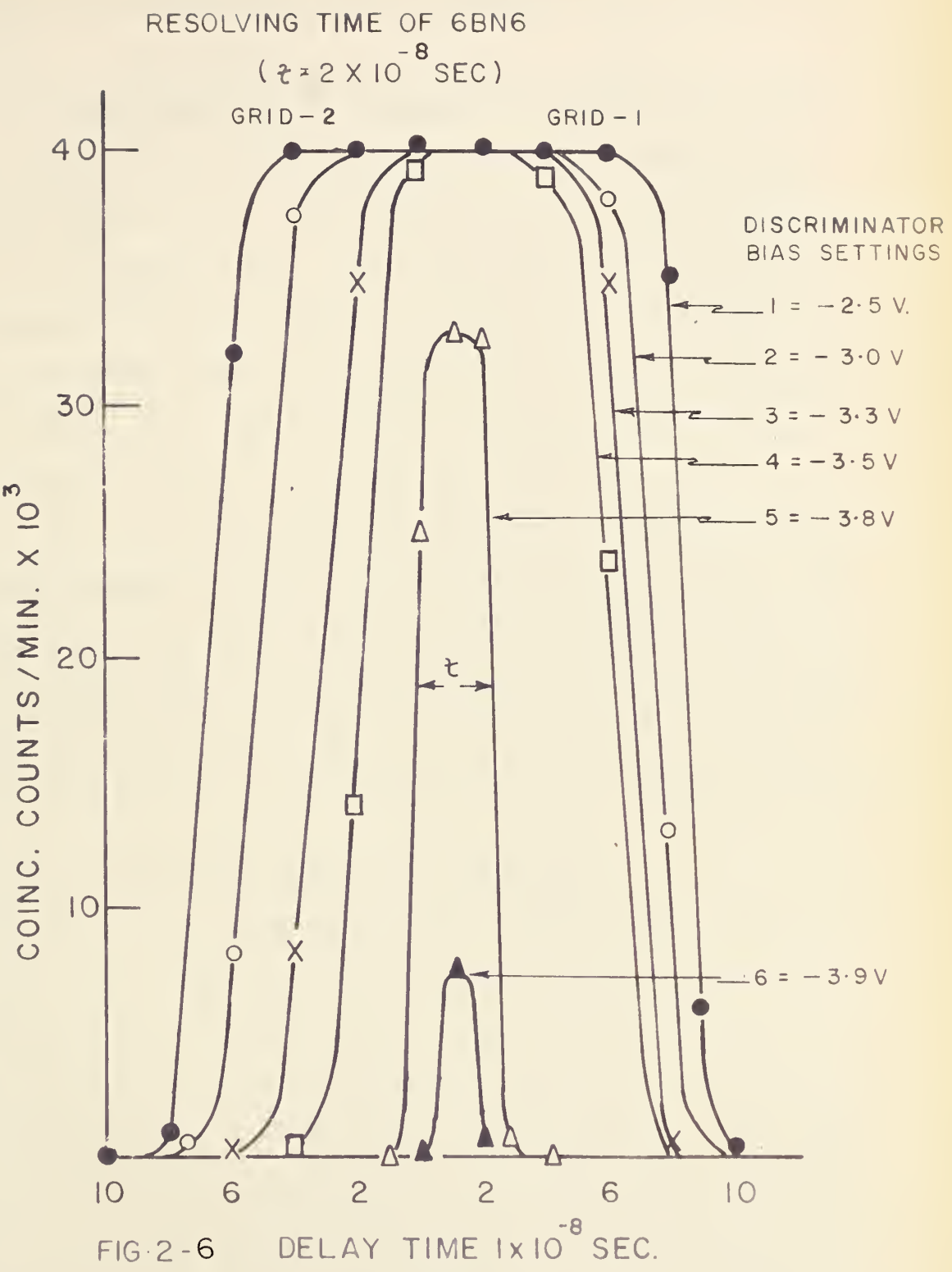
RESOLVING TIME OF 6BN6
(τ = 2 X 10⁻⁸ SEC)
GRID – 2
GRID – 1
40
30
20
10
COINC. COUNTS / MIN. X 10³
DISCRIMINATOR BIAS SETTINGS
1 = – 2·5 V.
2 = – 3·0 V
3 = – 3·3 V
4 = – 3·5 V
5 = – 3·8 V
6 = – 3·9 V
τ
10
6
2
2
6
10
DELAY TIME 1 x 10⁻⁸ SEC.

FIG·2-6

bringing the resolving time of the 6BN6 circuit to 2 x 10^{-8} second.

The resolving time is measured by delaying one input with respect to the other by a known amount and noting the coincidence count rate as a function of this delay time as is shown in Fig. 2-6. The signals are delayed by placing different lengths of RG 63U delay cable in series with the grid; each length corresponding to a known delay time. This process was repeated for each of the discriminator bias settings illustrated in Fig. 2-6. It is observed that the maximum counting rate remains constant between -2.5 V to 3.5 V bias values. The maximum counting rate of setting 5 is reduced to 90% of the counting rates at the lower bias values. At this bias setting the resolving time is 2 x 10^{-8} second. This bias value is taken to be the setting of the coincident circuit.

4. Slow Coincidence Figs. 2-7, 2-8, 2-9

The slow coincidence circuit, schematically shown in Fig. 2-7, consists of two separate input channels, a 6BN6 coincidence mixer, and an output channel. The input channel (Fig. 2-8) contains a phase inverter V1, a threshold amplifier V2a, V2b, and a trigger circuit V3 and V4. The 6BN6 coincidence circuit (Fig. 2-9) is the same as that outlined in the discussion of the fast coincidence circuitry. The output channel (Fig. 2-9)

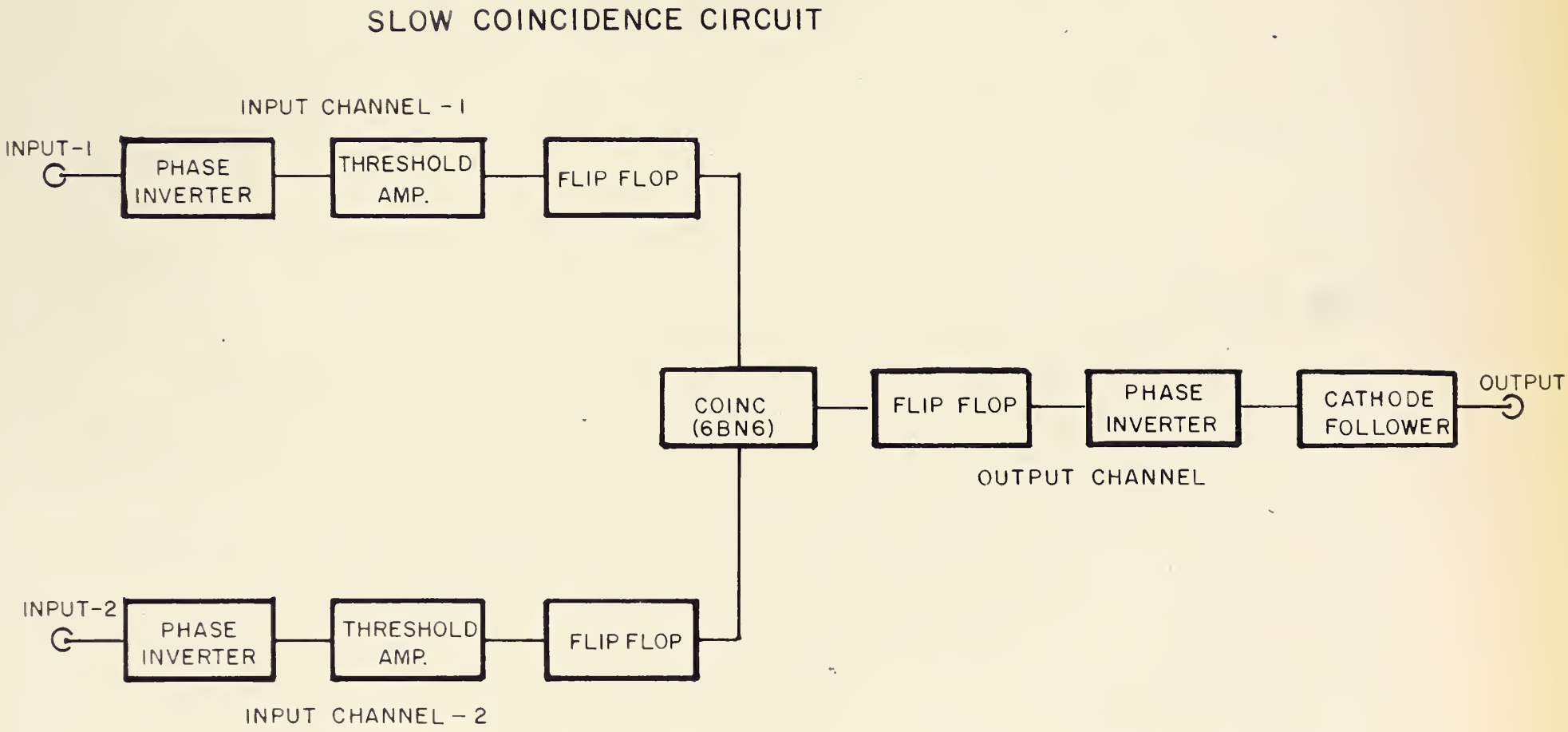
SLOW COINCIDENCE CIRCUIT
INPUT CHANNEL - 1
INPUT-1
PHASE INVERTER
THRESHOLD AMP.
FLIP FLOP
COINC (6BN6)
FLIP FLOP
PHASE INVERTER
CATHODE FOLLOWER
OUTPUT
OUTPUT CHANNEL
INPUT-2
PHASE INVERTER
THRESHOLD AMP.
FLIP FLOP
INPUT CHANNEL - 2

FIG. 2-7

INPUT CHANNEL

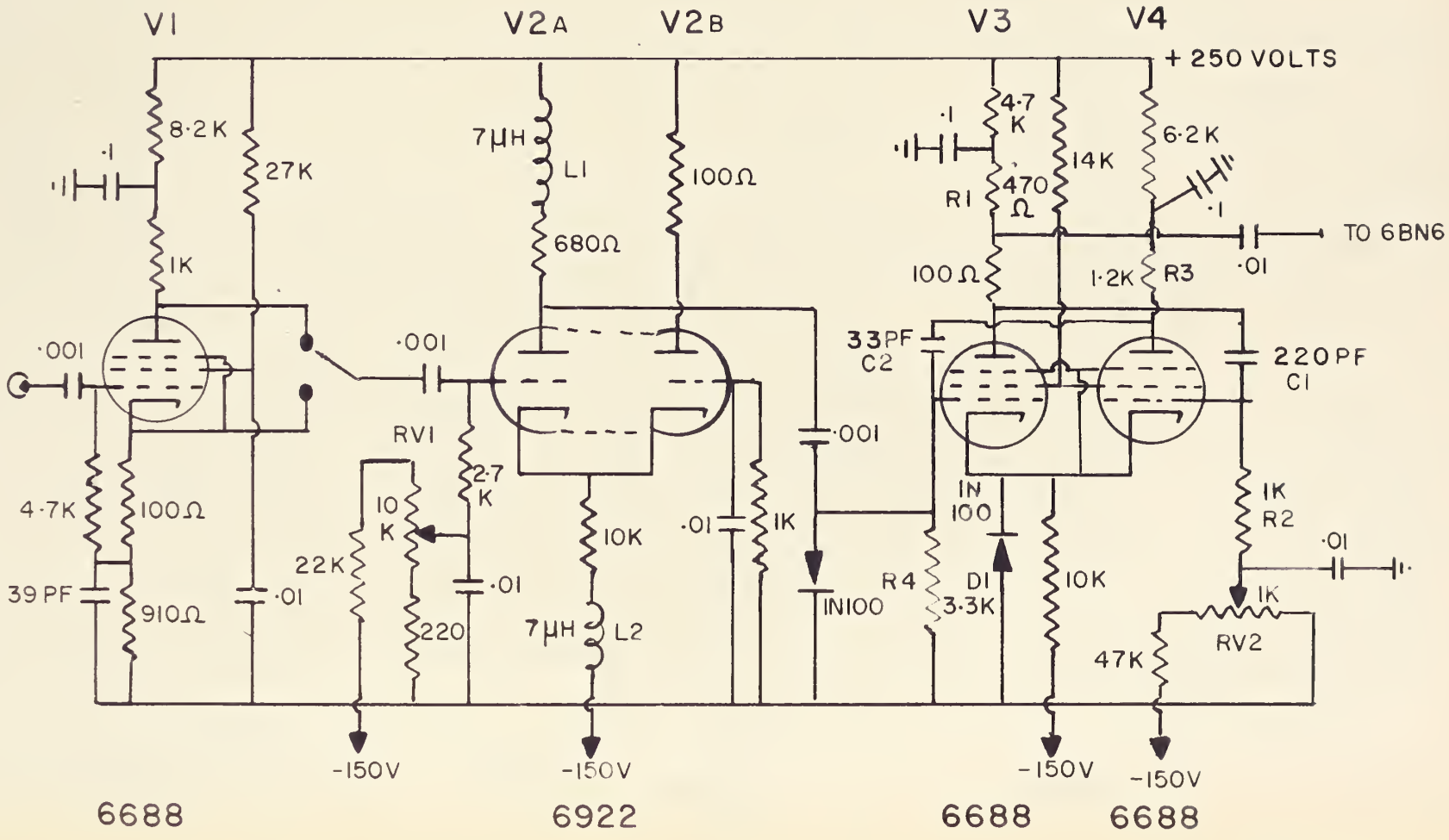

FIG. 2-8

COINCIDENCE AND OUTPUT CHANNEL

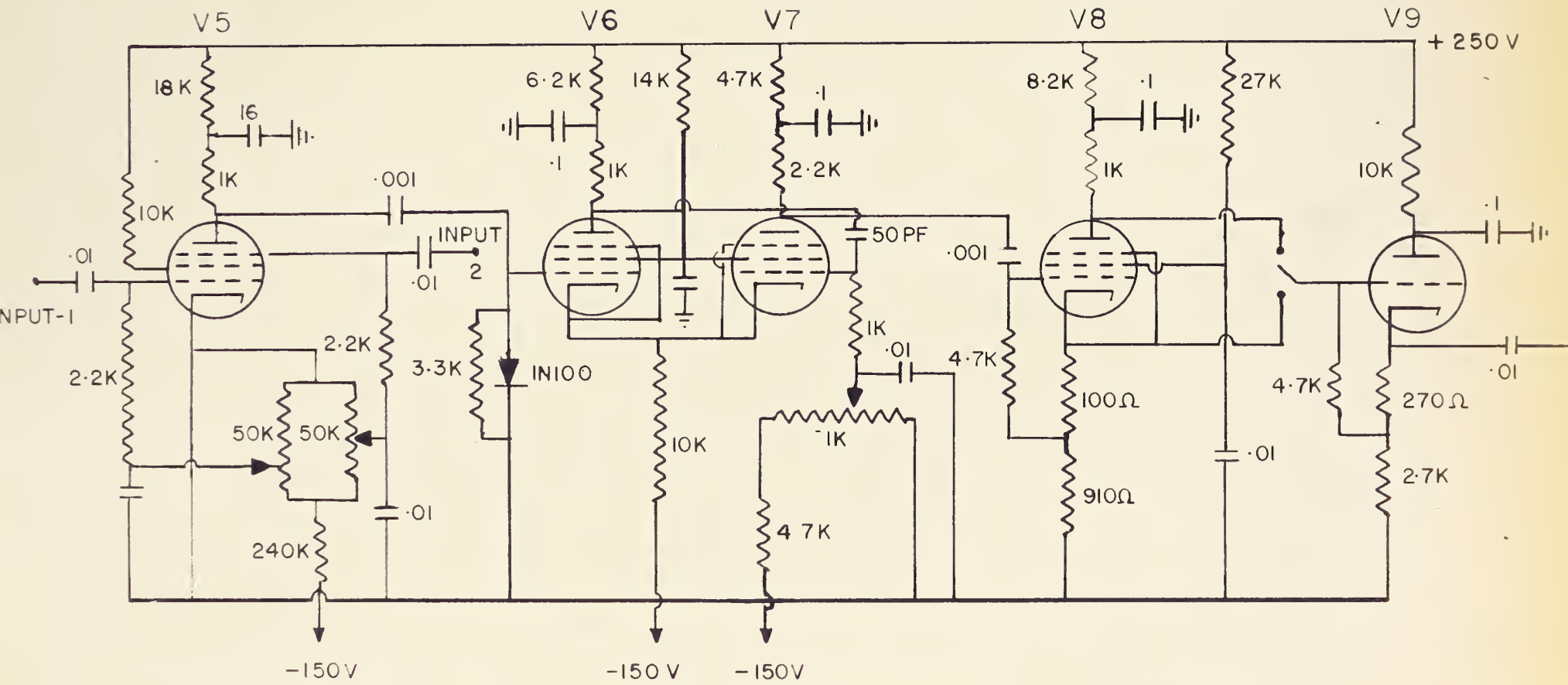

FIG. 2-9

contains a trigger circuit V5 and V6, a phase inverter V7 and a cathode follower V8. The input channels are sensitive to pulses of amplitude greater than 0.25 volts of both positive and negative polarity, the output channel produces pulses 10 volts in amplitude and 1-1/2 microsecond in length.

By having the plate resistor and the cathode resistor of V1 of equal value pulses with equal amplitude but with opposite phase are obtained from the plate and cathode in order to accept input pulses of either positive or negative polarity. The phase inverter is necessary to ensure that the input pulse to the threshold amplifier is positive.

The tube V2a of the treshold amplifier is normally cut off and V2b is normally conducting. A positive pulse on the grid of V2a drives it to conduction, transferring the current from V2b to V2a, resulting in a negative pulse on the plate of V2a. The potentiometer RV1 sets the threshold bias level above which the pulses are amplified with a gain of one and below which the pulses are not transmitted. The grid of V2b is decoupled to ensure that V2b has constant grid potential. 7 μh chokes L_2, L_4 are inserted in the common cathode circuit and the anode citcuit of V2a to increase the high frequency response

of the amplifier. The cathode choke makes the current transfer faster and the anode choke drives V2a into conduction more quickly. The advantage of this type of discriminator over the ordinary biased amplifier is the faster response and greater stability. The negative output of the threshold amplifier is used to trigger the "flip-flop" circuit.

The flip-flop circuit is a cathode coupled Schmitt trigger circuit which is triggered by a negative pulse. Under normal conditions V3 conducts and V4 is cut off. A negative pulse cuts off V3 raising the voltage on its plate. This positive pulse appears via C_1 on grid of V4 causing it to conduct heavily. The heavy conduction of V4 raises the common cathode potential, thus keeping V3 cut off. As the potential of the grid of V4 recovers exponentially toward a steady state value, the cathode potential decreases to a value which is sufficient to permit V3 to conduct. When V3 is turned on V4 is cut off sharply by the negative pulse which appears on the grid of V4 via C_1 from plate of V3. The controlling time constant is R_2C_1 which determines the length of the flip-flop cycle. The sensitivity of this trigger circuit is set by the potentiometer RV2 which adjusts the bias value of the grid of V4. This type of circuit is

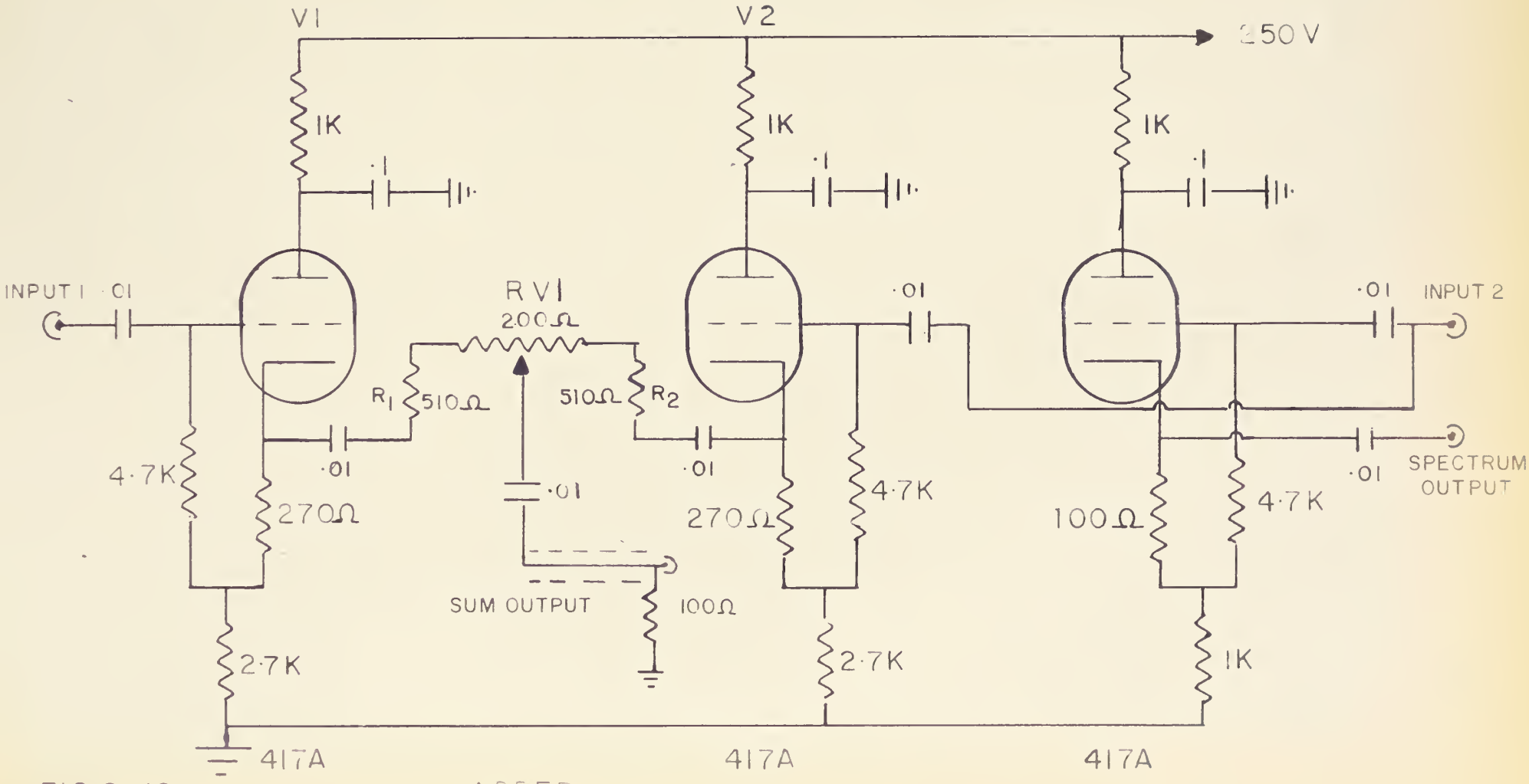

FIG. 2-10 ADDER BUFFER

satisfactory for producing pulses 1 to 2 microsecond long as was needed to activate the output channel flip-flop. To have a 100 nanosecond flip-flop pulse C_1 would be reduced to 20 pf. At this value of capacitor the back end of trigger pulse, however, has a long exponential decay which is undesirable. To remove this decay, a speed-up capacitor C_2 is inserted between the plate of V4 and the grid of V3 and a clamping diode between the cathode and ground and C_1 is increased to 220 pf. The effect of the speed-up capacitor is to cut off V3 harder while keeping the cathode clamped with D1. R_4C_2 becomes the controlling time constant for this modification.

The output signal is taken from the plate of V3 in order to have a positive necessary for the 6BN6 coincidence circuit which is the same as the fast coincidence circuit already described. The output of 6BN6 triggers the output flip-flop which produces a negative 10 volts, 1 microsecond pulse. This is inverted by the phase inverter V7 and driven out by the cathode follower V8.

5. Adding Circuit Fig. 2-9

The adding circuit is composed of two cathode followers V1 and V2, resistors R1 and R2 and potentiometer RV1. The potentiometer RV1 acts as a fine adjustment for the pulse size distribution of the two input pulses. The inputs from the two detectors are current-added to form a

not. The base line E is variable between 0 to 100 volts and the window width Δ E may be set from 0 to 10 volts.

Gate

The gate is a gated biased amplifier developed by Jones (Jr). It is possible to select coincidence or anticoincidence gating, coincidence gating requiring a 10 volt positive pulse to open the gate.

Multi-Channel Analyzer

The multi-channel analyzer is 100 channels analyzer type 1438B built by Philips Balham Works Ltd. The analyzer or "kicksorter" sorts a particular pulse height into a particular channel. The pulse height necessary to span the 100 channel is from 2 to 27 volts, the voltage difference per channel being 0.25 volts. The dead time, defined as the time interval during which the circuitry is inactive, of the kicksorter is 700 microseconds; and the maximum counting rate per channel is 40 counts per second with a count loss of 1%.

III. EFFICIENCY AND RESOLUTION OF THE SPECTROMETER

1. Efficiency

Absolute Efficiency

In order to establish the capabilities and usefulness of a spectrometer a knowledge of its efficiency is necessary. Before developing the analytic expression for the Hoogenboom spectrometer, one needs to know the efficiency of the detector itself. The total detection efficiency ε_t of a gamma ray detector is defined as the ratio of the number of gamma rays of energy E detected, $N_\gamma(E)$, to the total number, N_O, of gamma rays of energy E emitted by the source (Mo). If ω is the solid angle in spheres subtended by the detector at the point source, then

$$\varepsilon_t = \frac{N_\gamma(E)}{N_O \omega} \qquad (1\text{-}1)$$

This assumes that the source emits gamma rays isotropically. The absolute efficiency ε is defined as the product of solid angle and the total detection efficiency. Thus

$$\varepsilon = \frac{N_\gamma(E)}{N_O} \qquad (1\text{-}2)$$

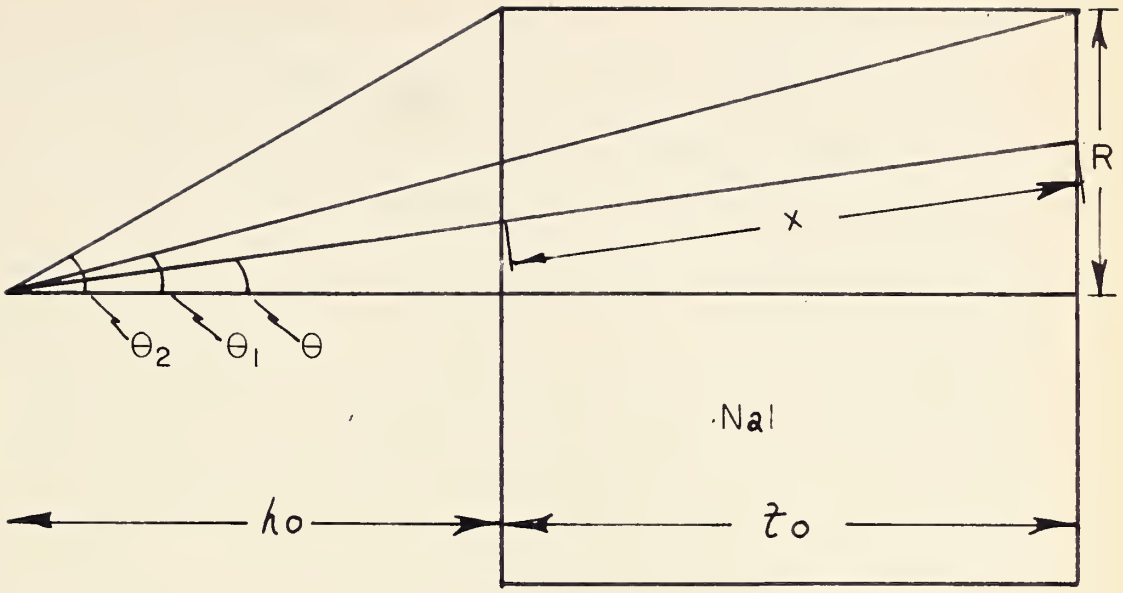

FIG. 3-1 GEOMETRY FOR CALCULATING THE EFFICIENCY OF AN UNCOLLIMATED CRYSTAL

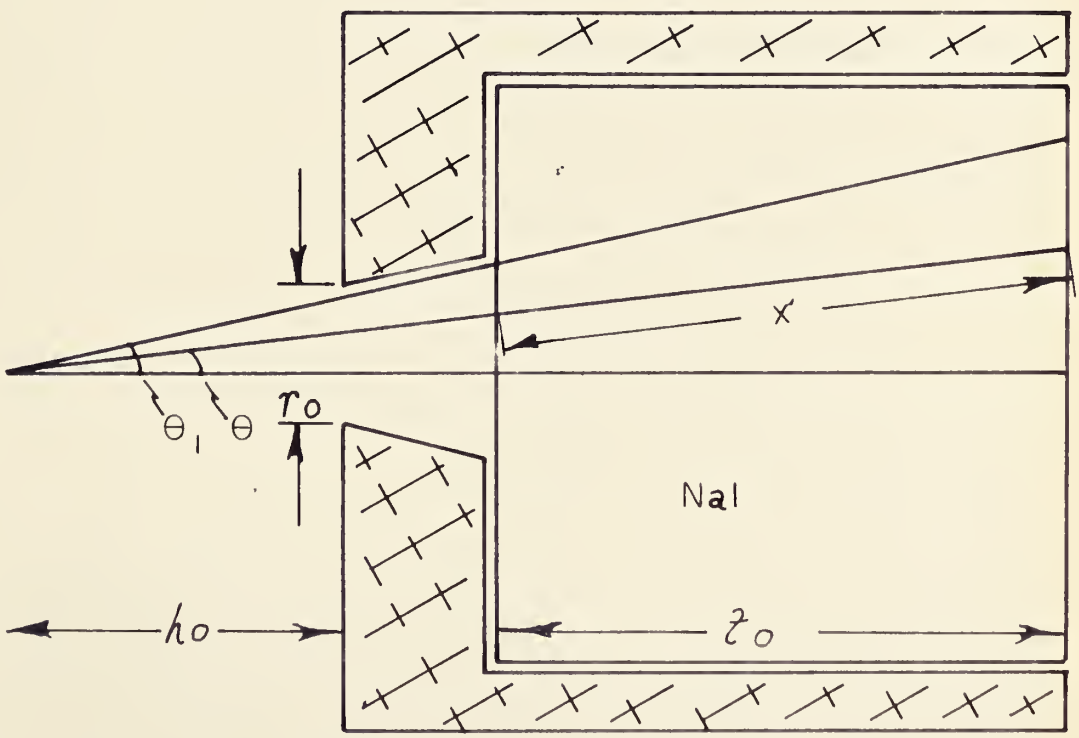

FIG. 3-2 GEOMETRY FOR CALCULATING THE EFFICIENCY OF A COLLIMATED CRYSTAL

sum current flowing to the output. The resistors R_1, R_2 are chosen to be ten times the output impedance of the cathode followers. Each resistor presents a high impedance path for the current driven from the opposite cathode follower, thus effectively the currents are added at the output.

In the buffer stage, a cathode follower isolates the spectrum signal from the adding network and prevents overloading the cathode follower feeding the long trans mission cable through which the spectrum pulse reaches the multi-channel analyzer.

6. The Remaining Electronic Equipment Fig. 2-1

Linear Amplifier 1

The linear amplifier 1 is a model 343 available from Franklin Electric Co. The amplifier accepts only negative pulses and has an input impedance of 100Ω, a gain of 1,000, and a maximum output pulse height of 100 volts.

Linear Amplifier 2

This amplifier is a Baird Atomic Linear Amplifier model 204B with a maximum gain of 15,000. and a maximum output pulse height of 100 volts.

Differential Discriminator

The differential discriminator or single channel pulse height analyzer is a model 510 produced by Atomic Instrument Co. Pulses with amplitude falling between E and E+ dE cause an output signal and all other pulses do

In the first expression 1-1 ε_t does not depend on the source-detector geometry whereas ε does. To obtain an expression for the absolute efficiency of a cylindrical crystal, consider the probability that a gamma ray will pass without interaction through NaI crystal of thickness x. This is $e^{-\mu x}$ where μ is the linear absorption coefficient. The probability that a gamma ray is absorbed is $1 - e^{-\mu x}$ and the number of gamma rays detected from an axial point source in a solid angle $d\omega$ is

$$dN(E) = N_0(1 - e^{-\mu x})d\omega.$$

The total number of gamma rays the uncollimated crystal detects is therefore

$$N(E) = N_0 \int_0^{\theta_2} (1 - e^{-\mu x}) 1/2 \sin\theta \, d\theta$$

where θ is the angle defined in Fig. 3-1. Thus the absolute efficiency is given by

$$\varepsilon = \int_0^{\theta_2} (1 - e^{-\mu x}) 1/2 \sin\theta \, d\theta \qquad (1\text{-}3)$$

where

$$x = t_0 \sec\theta \qquad 0 \le \theta \le \theta_1$$

or

$$x \sin\theta = R - h_0 \tan\theta \qquad \theta_1 \le \theta \le \theta_2$$

$$x = R \operatorname{cosec}\theta - h_0 \sec\theta$$

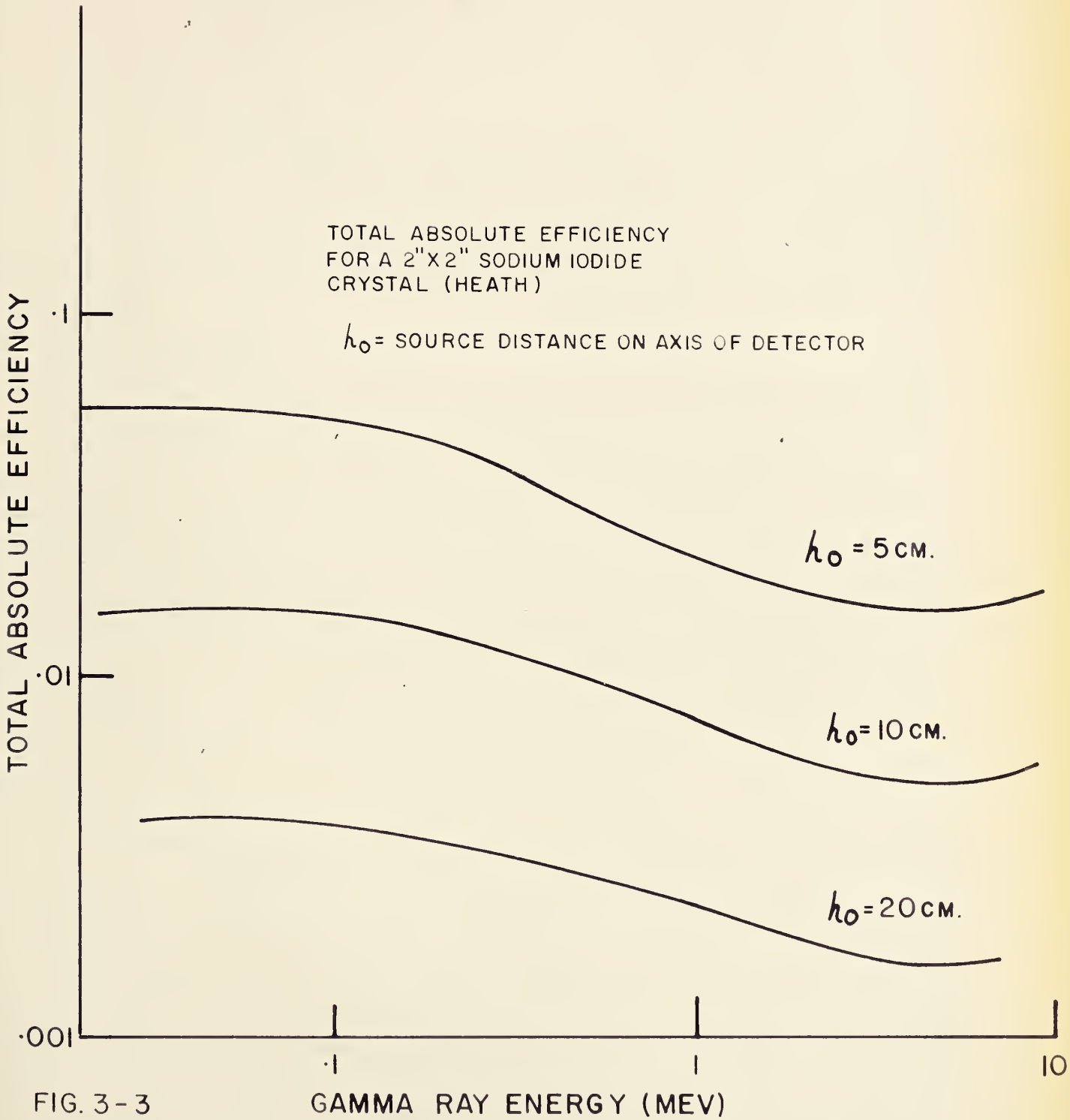
TOTAL ABSOLUTE EFFICIENCY
FOR A 2"X2" SODIUM IODIDE
CRYSTAL (HEATH)
h_0 = SOURCE DISTANCE ON AXIS OF DETECTOR
TOTAL ABSOLUTE EFFICIENCY
·1
·01
·001
h_0 = 5 CM.
h_0 = 10 CM.
h_0 = 20 CM.
·1
1
10
GAMMA RAY ENERGY (MEV)

FIG. 3-3

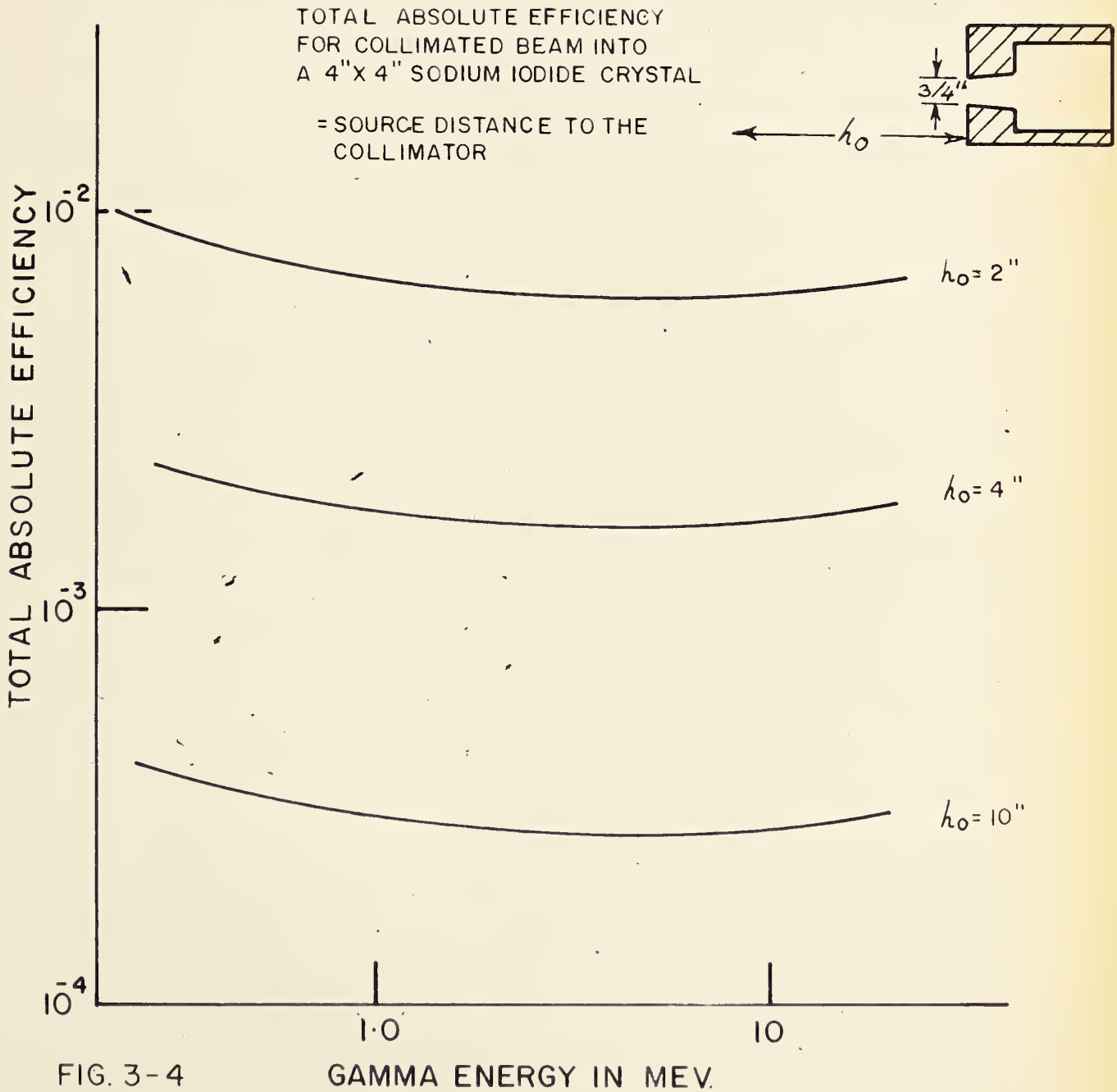
TOTAL ABSOLUTE EFFICIENCY
FOR COLLIMATED BEAM INTO
A 4"X 4" SODIUM IODIDE CRYSTAL
= SOURCE DISTANCE TO THE
COLLIMATOR
3/4"
h_o
TOTAL ABSOLUTE EFFICIENCY
10^{-2}
1
h_o= 2"
h_o= 4"
10^{-3}
h_o= 10"
10^{-4}
1·0
10
GAMMA ENERGY IN MEV.

FIG. 3-4

In the case of the collimated detector shown in Fig. 3-2, the absolute efficiency may be determined by

$$\varepsilon = \int_0^{\tan^{-1}\frac{r_o}{h_o}} \left(1 - e^{-\mu t_o \sec\theta}\right) \frac{1}{2} \sin\theta d\theta \qquad (1\text{-}4)$$

This expression assumes no scattering from the collimator; an added term is necessary to make the expression complete. This term, however, is expected to be small for a well collimated beam, and has not been considered in the calculation for the 4" NaI crystal shown in Fig. 3-3.

The efficiency of uncollimated NaI detector has been calculated by Heath (Hea) for 2" x 2" and 3" x 3" cylindrical crystals (Fig. 3-4). Efficiency curves for a 4" x 4" NaI collimated crystal has been calculated using expression 1-4. The values of $\mu(E)$ used are those given by Siegbahn (Sia), and are reproduced in the appendix.

The total detection efficiency as a function of gamma energy can be measured experimentally by two methods. A direct way to determine ε_t is to measure the total counting rate of a detector and the solid angle subtended by a source of known strength N_o, then to calculate ε_t from expression 1-1. If N_o is unknown, then the total detection efficiency can be obtained by a coincidence method (Si b). This method, however, is only

applicable to sources which emit cascading gamma rays. Using two identical NaI crystals subtending the same solid angle ω at the source, coincidence counting rate $N_{\gamma\gamma}$ is given by

$$N_{\gamma_1\gamma_2} = 2 N_0 \varepsilon_{t1} \varepsilon_{t2} \omega^2$$

where N_0 is the disintegrating rate and ε_{t1} and ε_{t2} are the total detection efficiencies for detecting γ_1 and γ_2 respectively. The single crystal counting rate N_γ is

$$N_\gamma = N_0 \omega (\varepsilon_{t1} + \varepsilon_{t2})$$

and the ratio of coincidence counting rate to the single crystal counting rate is

$$\frac{N_{\gamma_1\gamma_2}}{N_\gamma} = \frac{2 \varepsilon_{t1} \varepsilon_{t2}}{\varepsilon_{t1} + \varepsilon_{t2}} \cdot \omega \qquad (1\text{-}5)$$

The energies from the cascade gamma rays of Co^{60} are 1.17 Mev and 1.33 Mev, which are approximately equal so that $\varepsilon_{t1} \simeq \varepsilon_{t2}$ In which case

$$\frac{N_{\gamma_1\gamma_2}}{N_\gamma} = \varepsilon_{t1} \omega$$

The above expressions do not take into account the possibility of an anisotropic angular correlation between the gamma rays. Co^{60} is strongly correlated about 90°, the two detectors, however, are placed at 0° and 180° tending to cancell.e the anisotropy and making the expressions valid within 10%. To determine the efficiency at other energies it

is necessary to use a source in which one of the cascade gammas is 1.2 Mev and the other of some different value. Such a source is Na^{22} which emits 1.28 Mev and 0.51 Mev coincident gamma rays. Using the efficiency determined from Co^{60} the total detection efficiency may be determined. To avoid coincidence between the annihilation quanta, the detectors must not be placed such that the source lies near a line joining the detectors.

Photo Peak Efficiency

The photo peak efficiency is defined as the ratio of the number of counts N_p in the photo peak (more properly called full energy peak, where large crystals are involved) to the number of gamma rays of energy E emitted by the source (M_o). Thus

$$\varepsilon_p = \frac{N_p(E)}{N_o} \qquad (2\text{-}1)$$

ε_p depends on geometry in the same way as ε . The a priori probability that a photon may be completely absorbed in dy at distance y from the point of entry of the crystal is the product of the probability $e^{-\mu y}$ of reaching y without interaction and τ dy the probability of total absorption in dy. τ is the "effective photo-electric absorption coefficient," though it contains terms pertaining to multiple processes leading to the complete

absorption as well to the photoelectric effect. The efficiency $\varepsilon_p(E)$ is, therefore, given by

$$\varepsilon_p = 1/2 \int_0^{\theta_2} \sin\theta d\theta \int_0^x \tau e^{-\mu y} dy \qquad (2\text{-}2)$$

where θ and x are defined by the geometry. The value of τ is not easily determined theoretically because the complexity of calculations involving multiple interactions. The photo peak efficiency, however, can be determined experimentally by considering the ratio of the area under the photo peak to the total area under the spectrum and the absolute efficiency ε . Let the ratio of the areas be R, such that

$$R = \frac{N_p}{N_t} \qquad (2\text{-}3)$$

Then $\varepsilon_p = R\varepsilon_t$. By using the calculated values of ε_t and the measured values of R, ε_p can be calculated.

Hoogenboom Efficiency

To develop an expression for the efficiency of the Hoogenboom spectrometer consider for simplicity a nucleus which deexcites by two cascade gamma rays. Let γ_1 and γ_2 be the two cascade gammas with energies E_{o1} and E_{o2} respectively. Let $\rho_1(E_1)$ be the probability of recording γ_1 with energy E_1 in the gated spectrum. Assume the photo peak to have a gaussian distribution $f_1(E_1 - E_{o1})$

with standard deviation σ_1 and similarly for γ_2. Let $f_s^t(E_1+E_2-E_{0s})$ be the sum discriminator profile which is a rectangular profile of width Γ_s. Then the probability of detecting γ_1 of apparent energy in dE_1 at E_1 in coincidence with γ_2 of apparent energy in dE_2 at E_2 is given by

$$d\rho_1(E_1)\,dE_1 = f_1(E_1-E_{01})\,f_2(E_2-E_{02})\,f_s^t(E_1+E_2-E_{0s})\,dE_1\,dE_2$$

then

$$\rho_1(E_1)\,dE_1 = f_1(E_1-E_{01})\,dE_1 \int_0^\infty f_2(E_2-E_{02})\,f_s^t(E_1+E_2-E_{0s})\,dE_2 \qquad (3\text{-}1)$$

The diagram below shows the distributions of the gamma rays together with the sum profile under consideration.

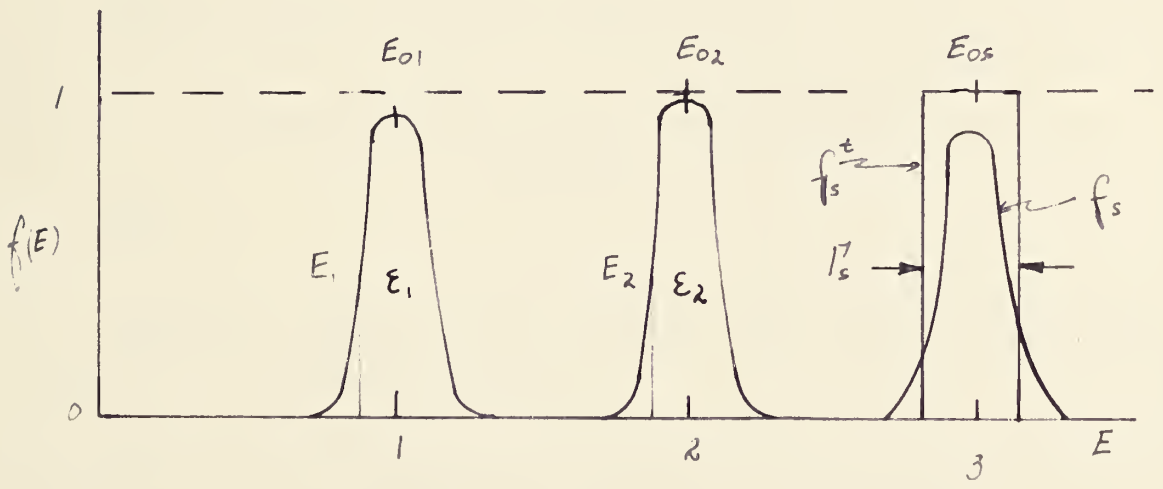

The sum profile f_s^t is given by

$$f_s^t = 1 \qquad E_{0s} - \frac{\Gamma_s}{2} \leq E_1 + E_2 \leq E_{0s} + \Gamma_s/2$$

$$= 0 \qquad \text{elsewhere}$$

For ease of calculation consider, however, the sum profile to be approximated by a gaussian distribution f_s with standard deviation σ_s such that

$$\Gamma_s = \int_0^{\infty} f_s^{t} \, dE_1 \, dE_2 = \int_0^{\infty} f_s \, dE_1 \, dE_2$$

Then

$$P_1(E_1)\, dE_1 = f_1(E_1 - E_{01})\, dE_1 \int_0^{\infty} f_2(E_2 - E_{02})\; f_s(E_1 + E_2 - E_{0s})\, dE_2$$

Taking the distribution functions to be given by

$$f_{1,2}(E_{1,2} - E_{01,2}) = \frac{\varepsilon_{1,2}}{\sigma_{1,2}\sqrt{2\pi}} \; e^{-\frac{(E_{1,2} - E_{01,2})^2}{2\sigma_{1,2}}}$$

where $\varepsilon_{1,2}$ is the photo peak efficiency of detecting $\gamma_{1,2}$ which is given by

$$\varepsilon_{1,2} = \int_0^{\infty} f_{1,2}\, dE_{1,2}$$

The sum distribution is taken to be

$$f_s(E_1 + E_2 - E_{0s}) = \frac{\Gamma_s}{\sigma_s \sqrt{2\pi}} \; e^{-\frac{(E_1 + E_2 - E_{0s})^2}{2\sigma_s^2}}$$

Then

$$P_1(E_1)\, dE_1 = \frac{\varepsilon_1 \varepsilon_2 \Gamma_s \, dE_1}{\sigma_1 \sigma_2 \sigma_s (2\pi)^{3/2}} \int_0^{\infty} e^{-\frac{1}{2}\left[\frac{(E_1 - E_{01})^2}{\sigma_1^2} + \frac{(E_2 - E_{02})^2}{\sigma_2^2} + \frac{(E_1 + E_2 - E_{0s})^2}{\sigma_s^2}\right]} dE_2$$

The Hoogenboom efficiency for recording γ_1 is

$$\varepsilon_{1s} = \int_0^{\infty} P_1(E_1)\, dE_1 \qquad (3\text{-}2)$$

A convenient change of variables is

$$x = E_1 - E_{01} \qquad dx = dE_1$$

$$y = E_2 - E_{02} \qquad dy = dE_2$$

Then

$$\mathcal{E}_{1S} = \frac{\mathcal{E}_1 \mathcal{E}_2 \Gamma_S}{\sigma_1 \sigma_2 \sigma_S (2\pi)^{3/2}} \int_0^\infty e^{-\frac{x^2}{2\sigma_1^2}} \int_0^\infty e^{-\frac{y^2}{2\sigma_2^2}} \cdot e^{-\frac{(x+y)^2}{2\sigma_S^2}} \, dx\, dy$$

Consider the integrand

$$e^{-\frac{1}{2}\left[x^2/\sigma_1^2 + y^2/\sigma_2^2 + (x+y)^2/\sigma_S^2\right]}$$

If the inside bracket is expanded, the exponent becomes

$$x^2/\sigma_1^2 + y^2/\sigma_2^2 + x^2/\sigma_S^2 + y^2/\sigma_S^2 + 2xy/\sigma_S^2$$

$$= x^2\left(1/\sigma_1^2 + 1/\sigma_S^2\right) + y^2\left(1/\sigma_2^2 + 1/\sigma_S^2\right) + 2xy\left(1/\sigma_S^2\right)$$

$$= x^2\left[\frac{\sigma_1^2 + \sigma_2^2 + \sigma_S^2}{\sigma_1^2(\sigma_2^2 + \sigma_S^2)}\right] + \left[y + \frac{\sigma_2^2 x}{\sigma_2^2 + \sigma_S^2}\right]^2 \left[\frac{\sigma_2^2 + \sigma_S^2}{\sigma_2^2 \sigma_S^2}\right]$$

Replacing the lower limit of integration by $-\infty$ changes the value of the integral very little since in practical cases $E \gg \sigma$. Integrating over y first the integral becomes

$$p_1(x) = \frac{\mathcal{E}_1 \mathcal{E}_2 \Gamma_S}{2\pi\sigma_1\left(\sigma_2^2 + \sigma_S^2\right)^{1/2}} \, e^{-x^2\left[\frac{\sigma_1^2 + \sigma_2^2 + \sigma_S^2}{2\sigma_1^2(\sigma_2^2 + \sigma_S^2)}\right]} \qquad (3\text{-}4)$$

Integrating over x the Hoogenboom efficiency becomes

$$\varepsilon_{1s} = \varepsilon_1 \varepsilon_2 \Gamma_s / (2\pi)^{1/2} \left(\sigma_1^2 + \sigma_2^2 + \sigma_s^2\right)^{1/2} \qquad (3\text{-}5a)$$

Because the order of integration of x and y can be reversed the efficiency for detecting γ_2 is also given by

$$\varepsilon_{2s} = \varepsilon_1 \varepsilon_2 \Gamma_s / (2\pi)^{1/2} \left(\sigma_1^2 + \sigma_2^2 + \sigma_s^2\right)^{1/2} = \varepsilon_{1s} \qquad (3\text{-}5b)$$

It, therefore, follows that the areas under the full energy peaks in the Hoogenboom spectrum are equal, provided the sum differential discriminator window is centered on the sum peak.

A more exact expression for the efficiency for the Hoogenboom spectrometer is obtained using the actual rectangular profile of the sum discriminator window rather than the gaussian distribution which has been used for simplicity.

Then

$$p_1(x)\,dx = \frac{\varepsilon_1 \varepsilon_2 \Gamma_s}{2\pi \sigma_1 \sigma_2} e^{-\frac{x^2}{2\sigma_1^2}} dx \int_{-x-\frac{\Gamma_s}{2}}^{-x+\frac{\Gamma_s}{2}} e^{-y^2/2\sigma_s^2} dy$$

and the Hoogenboom efficiency becomes

$$\varepsilon_{1s} = \frac{\varepsilon_1 \varepsilon_2 \Gamma_s}{2\pi\sigma_1\sigma_2} \int_0^\infty e^{-x^2/2\sigma_1^2} \left[\operatorname{erf}\left(x - \frac{\Gamma_s}{2}\right) + \operatorname{erf}\left(x + \frac{\Gamma_s}{2}\right) \right] dx \quad (3\text{-}6)$$

The photo peak resolution of a scintillation detector is defined to be the full width Γ of the peak at half the maximum, expressed as a percentage of the peak abscissa. Thus far the standard deviation σ has been considered as a measure of resolution. To relate Γ to the standard deviation σ consider a standardized guassian distribution $\varphi(u) = e^{-u^2/2}$

where $u = x/\sigma$

at maximum $\varphi(0) = 1$

at half maximum $\varphi(u) = 1/2 = e^{-1/2\, u^2}$

$$\therefore \quad u = \pm (2 \ln 2)^{1/2}$$

$$\Gamma = 2|\mu|$$

$$\therefore \Gamma = \sigma (8 \ln 2)^{1/2}$$

The Hoogenboom efficiency in terms of Γ is, therefore,

$$\varepsilon_{1s} = \varepsilon_1 \varepsilon_2 \Gamma_s \left(\frac{4 \ln 2}{\pi}\right)^{1/2} / \left(\Gamma_1^2 + \Gamma_2^2 + \Gamma_s^2\right)^{1/2} \quad (3\text{-}7)$$

The table below shows the calculated and measured absolute efficiency for 4" NaI crystal collimated at a source distance of 4 inches. The ratio R is determined by counting the squares under the total spectrum, the squares under the photo peak and taking the ratio of the two areas. The experimental Hoogenboom efficiency was obtained by considering the counting rate of the photo peak and dividing it by the total counting rate of the crystal i.e.

$$\varepsilon_s = \frac{N_{\alpha_1 \gamma_2}}{N_\gamma} (\varepsilon_1 + \varepsilon_2)$$

Energy	0.51 Mev.	0.667 Mev.	1.17 Mev.
Source	Na^{22}	Cs^{137}	Co^{60}
ε Measured $\pm$ 5%	3.8×10^{-3}		3.6×10^{-3}
$R = \frac{N_p}{N_t}$ $\pm$ 3%	0.68	0.66	0.43
$\varepsilon_p = R\,\varepsilon$ $\pm$ 8%	2.6×10^{-3}		1.56×10^{-3}
ε Calculated $\pm$ 2%	2.10×10^{-3}	1.99×10^{-3}	1.85×10^{-3}
ε_s Measured $\pm$ 5%	1.7×10^{-6}		1.6×10^{-6}
ε_s Calculated $\pm$ 5%	1.4×10^{-6}		1.3×10^{-6}

2. Resolution

The resolution of a photo peak is defined to be the full width of the peak at half the maximum, expressed as a percentage of the peak abscissa. The resolution of the Hoogenboom spectrometer is determined by the resolution of each separate crystal, the width of the sum channel discriminator window, and the resolving time of the circuitry.

The crystal resolution (Sic) is affected by the fluorescence efficiency and light collection efficiency. For good resolution the number of optical photons emitted per Mev of energy loss in the crystal should be large and constant throughout the crystal. The light should be emitted in a wavelength range to which the photo cathode of the photomultiplier is most sensitive. The crystal must be transparent to the light produced and must be contained in a reflecting housing. The photomultiplier must be joined to the window of the crystal housing in such a manner as to reduce light loss. The two are usually joined with silicone oil, which has the same refractive index as the glass surface covering the crystal and the face of the photomultiplier. To direct all the light to the photomultiplier, the housing of the crystal is coated with magnesium oxide, which has high reflectivity. These properties inherent in the crystal and its mounting to a large extent determine the resolution.

The photomultiplier affects the resolution of the

detectors through factors which include photo efficiency and uniformity of the photo cathode, photoelectron collection efficiency, dynode amplification, tube noise and fatigue effects. For good photo tubes these factors have a smaller effect on resolution than do the properties of the crystal.

The dead time of an electronic circuit is defined as the length of time after a pulse during which the circuitry is insensitive. Since all the pulse circuits have a finite dead time, all the detected pulses may not be recorded. The complete loss of pulses does not distort the spectrum, but pulses overlapping the end of this insensitive period are altered in shape, which results in incorrect recording. At high counting rates there is an effective reduction in efficiency because of the lost pulses. The true counting rate m and the observed counting rate n are simply related when there is a fixed dead time τ. The number of counts lost per second during the total dead time $m\tau$ is $mn\tau$ and the true counting rate m is given by

$$m = n + mn\tau \qquad \text{or} \quad m = \frac{n}{1 - \tau n}$$

In practice τ is measured by measuring the count rates n_1 and n_2 of two sources separately, then n_3 of the two sources simultaneously; τ is then easily calculated.

Because of the finite coincidence resolving time t, there is a finite probability that random pulses may cause an output pulse from the coincidence circuitry. If n_1 and

n_2 are two (unrelated) input rates, then it is easily shown that the chance coincidence rate n_c is given by $n_c = 2tn_1n_2$. For high counting rates it is, therefore, necessary to have as short a resolving time as possible to reduce the true count to chance count ratio. The reduction of background counting rates also improves the effective resolution. The resolving times of the fast and slow coincidence circuits are 2×10^{-8} sec. and 3×10^{-7} sec. respectively.

Resolution of the Hoogenboom Spectrometer

The expression for the resolution of the Hoogenboom spectrometer is obtained by considering two cascading gamma rays γ_1 and γ_2 of energy E_{o1} and E_{o2} respectively. The probability of detecting γ_1 with energy between E_1 and $E_1 + dE_1$ in coincidence with γ_2 of energy E_2 is given by expression (3-4)

$$p(E_1)\,dE_1 = \frac{\varepsilon_1 \varepsilon_2 \eta_s}{2\pi\sigma_1(\sigma_2^2+\sigma_s^2)^{1/2}} e^{-\frac{1}{2}(E_1-E_{o1})^2\left(\frac{\sigma_1^2+\sigma_2^2+\sigma_s^2}{\sigma_1^2(\sigma_2^2+\sigma_s^2)}\right)} dE_1$$

The equivalent standard deviation σ of the above expression is

$$\sigma_{s_1} = \frac{\sigma_1(\sigma_2^2+\sigma_s^2)^{1/2}}{(\sigma_1^2+\sigma_2^2+\sigma_s^2)^{1/2}} \qquad (4\text{-}1)$$

Using the relation $\Gamma = \sigma(8\ln 2)^{1/2}$ which relates the full width Γ to the standard deviation σ, the Hoogenboom full

width for γ_1 is

$$\Gamma_{s1} = \Gamma_1 \left(\Gamma_2^2 + \Gamma_s^2\right)^{1/2} / \left(\Gamma_1^2 + \Gamma_2^2 + \Gamma_s^2\right)^{1/2} \qquad (4\text{-}2)$$

It may be observed from the above expression that the full width of the Hoogenboom spectrum is narrower than the full width of the single crystal photo peak. By making the sum width Γ_s much narrower than either of the two single crystal widths, that is $\Gamma_s \ll \Gamma_1$ and $\Gamma_s \ll \Gamma_2$

$$\Gamma_{s1} \simeq \frac{\Gamma_1 \Gamma_2}{(\Gamma_1^2 + \Gamma_2^2)^{1/2}} \simeq \Gamma_{s2} \qquad (4\text{-}3)$$

The widths of the peaks in the Hoogenboom spectrum are approximately independent of energy provided that the sum window width is small enough. To see the energy E variation consider expression 4-3 in terms of E and E_s

$$\Gamma_{s1} \simeq \Gamma_1(E)\,\Gamma_2(E_s - E) / \left(\Gamma_1^2(E) + \Gamma_2^2(E_s - E)\right)^{1/2}$$

An approximate formula relating the photo peak width to the energy is $\Gamma \propto E^{1/2}$ then

$$\Gamma_{s1} \propto E^{1/2}(E_s - E)^{1/2} / (E + E_s - E)^{1/2}$$

$$\propto E^{1/2}\left(1 - E/E_s\right)^{1/2}$$

This is a slowly varying function of E except near zero and E_s. Because the widths remain nearly constant the improvement in resolution is greatest for the high energy member of the cascade. In the case where the two cascade gamma rays have nearly the same energy, there is an improvement by a factor of $\sqrt{2}$ over the single crystal resolution. Consider Co^{60} as an example. In this case $\Gamma_1 \simeq \Gamma_2 = 120$ Kev. If the sum channel is set to about 50 Kev width, then $\Gamma_{s_1} = \Gamma_2/\sqrt{2} = 80$ Kev or $\left(\frac{\Delta E}{E}\right)_{1.33\ Mev} = 6\%$ as compared to 9% for the single crystal.

IV. EXPERIMENTAL PROCEDURE

The 2" and 4" NaI(Tl) cylindrical crystals were purchased from the Harshaw Chemical Co. already housed in aluminum casings with glass windows. The crystals are mounted on RCA 6342 and 7046 photo tubes respectively in a manner calculated to obtain good optical contact between the glass window of the crystal and the photo tube, and to ensure that the system is light tight. The 2" crystal assembly is shown in Fig. 4-1 and the 4" crystal assembly in Fig. 4-2.

The optical joint for both crystals is made with Dow-Corning D.C.-200 silicone oil. The silicone oil is applied to the glass window of the crystal container and allowed to flow evenly over the surface. After all the air bubbles trapped in the oil have escaped, the photo tube is pressed on to the crystal in such a way that no air gaps form between the crystal and the photo tube. The 2" assembly is completed by wrapping several layers of electrical tape around the crystal and the photo tube. The 4" crystal assembly is mounted in a casing of soft iron which acts as a magnetic shield for the photo tube as well as supporting the crystal.

CRYSTAL MOUNTING

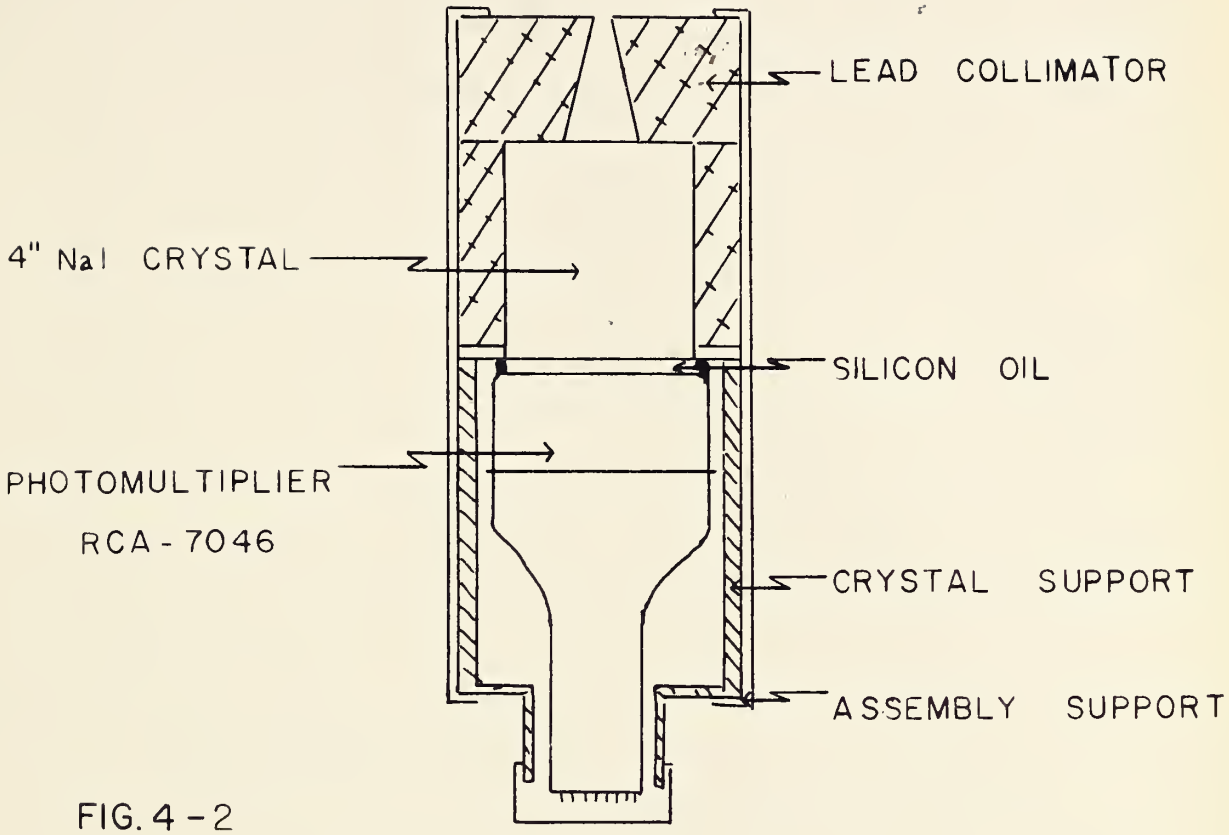

FIG. 4 - 2

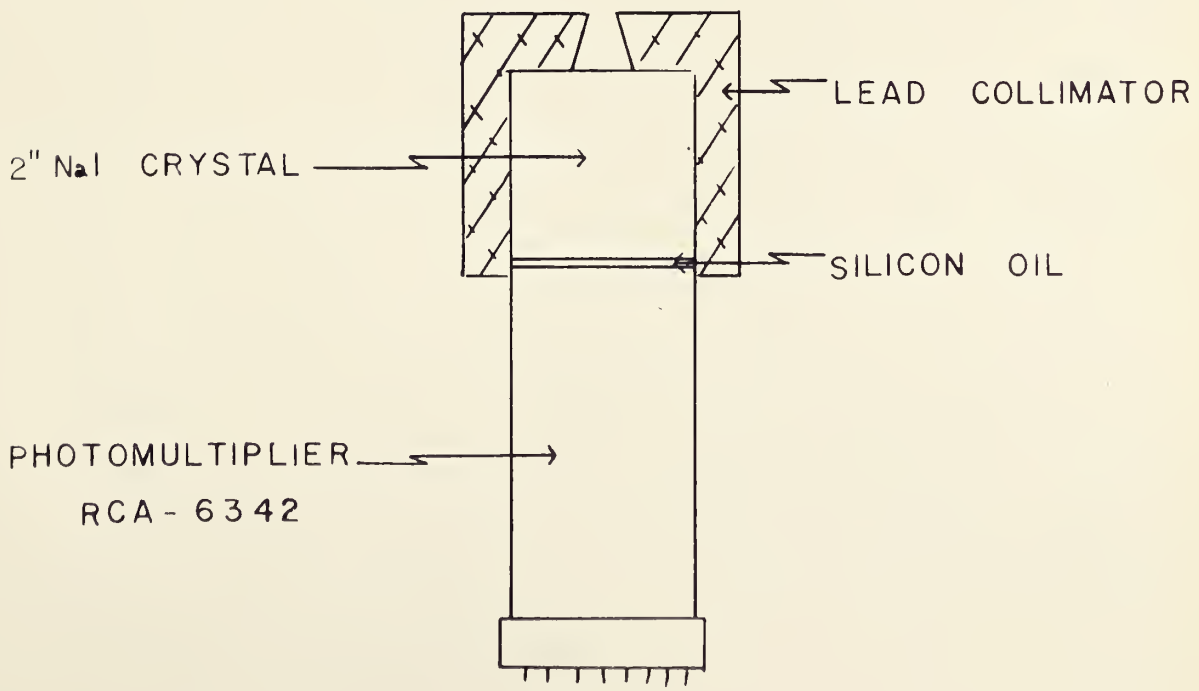

FIG. 4 - 1

The optical joint is checked periodically for good contact by measuring the resolution of a photo peak. For a good contact the resolution of the 4" crystals is 10% for the 1.28 Mev gamma ray from Na^{22}, whereas for a poor joint the resolution is noticeably poorer. To correct a poor joint the crystal window and photo tube are cleaned and the silicone oil reapplied. The detectors are checked for light leaks by directing a light beam successively at all points of the detector casing and observing the increase in noise output with an oscilloscope when light reaches the detector. The light leaks are repaired by applying several layers of electrical tape over the leaking area.

Spectrometer Alignment

In adjusting the spectrometer the anode voltage (H.T.) of each photo tube is adjusted to attain a standard energy calibration. RCA 6342 tubes are set near 1500 volts and the RCA 7046 tubes are near 2650 volts. When the energy calibration is set, pulses from the two tubes are compared at the adder input to ensure that they have identical shape. Corrections to the shape are made by adjusting the time constants $R_L C$ where R_L is the load resistor of the photo tube and C the coupling capacitor between the photo tube and the cathode follower. After the pulse shapes are adjusted the photo tubes are again calibrated in energy by displaying the spectrum of each detector on the kicksorter.

The output of the limiter and shaper of each detector is examined to see whether both limiters limit at the same input signal level and whether the output pulses are of the same size and shape. The limiters are set to limit at about 0.3 Mev by small adjustments of the photo tube H.T.; the output pulse heights are equalized by adjusting the potentiometers RV1 in the limiter and shaping circuit. The pulse length is preset by the length of clipping cable. The limiters are thus adjusted to give 100 nanosecond, 2.5 volt rectangular pulses.

The bias levels of the 6BN6, are adjusted by means of the potentiometers RV1 and RV2 in the fast coincidence circuit to obtain a compromise between maximum output pulse height and minimum "capacity" pulse height. For this adjustment the counters are set at 180^{o} and the coincident 0.51 Mev annihilation photons from Na^{22} are used.

The potentiometer RV1 in the adding circuit is adjusted to give a sum spectrum which, when displayed on the kicksorter, has a distribution similar to that of a single crystal. If the potentiometer is set incorrectly, a given photo peak in a single crystal spectrum corresponds to two separate peaks in the sum spectrum. The potentiometer is adjusted until the separate peaks are superimposed.

After the adding circuit and coincidence circuit are properly adjusted, the delay time between the spectrum pulse and the gating signal is measured using an oscilloscope triggered by the output of the 6BN6. The delay between the pulses is compensated by inserting appropriate lengths of RG65U delay cable in the signal paths to establish coincidence between the gate pulse and the spectrum pulse. The equipment is then ready for spectral analysis.

Spectrum Analysis

A gamma ray spectrum is analyzed by first displaying the single crystal spectrum and identifying the gamma rays present. After identifying the energy of the gamma rays the sum discriminator is set to a level corresponding to the sum of the energies of two gamma rays which are assumed to be cascading. This level is roughly adjusted by observing the pulse height at the input of the discriminator with an oscilloscope. With this base line setting, the window of the discriminator is opened wide and the Hoogenboom spectrum is gated onto the kicksorter. The photo peaks of the gated spectrum appear symmetrical if the base line is set at the proper value, or they appear distorted if it is not. For the incorrect base setting the displayed spectrum has a higher distribution of counts towards the position of the base setting. The base line is then moved in the direction which makes

the gated photo peak symmetric. Once the base line is set the window width is narrowed to the smallest value which does not distort the spectrum.

V. RESULTS AND DISCUSSION

1. Collimation

Gamma rays are collimated into the center of each crystal in order to increase the ratio of photo peak efficiency to total efficiency, R, and to reduce the detection of gamma rays which are back scattered from one crystal into the other. Collimation of the beam into the crystal increases the probability that a gamma ray is completely absorbed, since all gamma rays permitted to enter the crystal are forced to traverse the full thickness of the crystal. Complete absorption results in a count in a photo peak. When the gamma rays are not collimated then a large number of those incident near the edge of the crystal are Compton scattered out of the crystal, consequently increasing the area under the Compton distribution. Compton scattering therefore reduces R. Curve (1) of Fig. 4-1 is a Co^{60} spectrum from an uncollimated 4" NaI crystal; curve (4) is the same spectrum when the gamma rays are collimated by a 3/4" collimating hole in a 4" thick lead shield. It is seen from these curves that the Compton level has been reduced by about a factor of 2. The valley between the

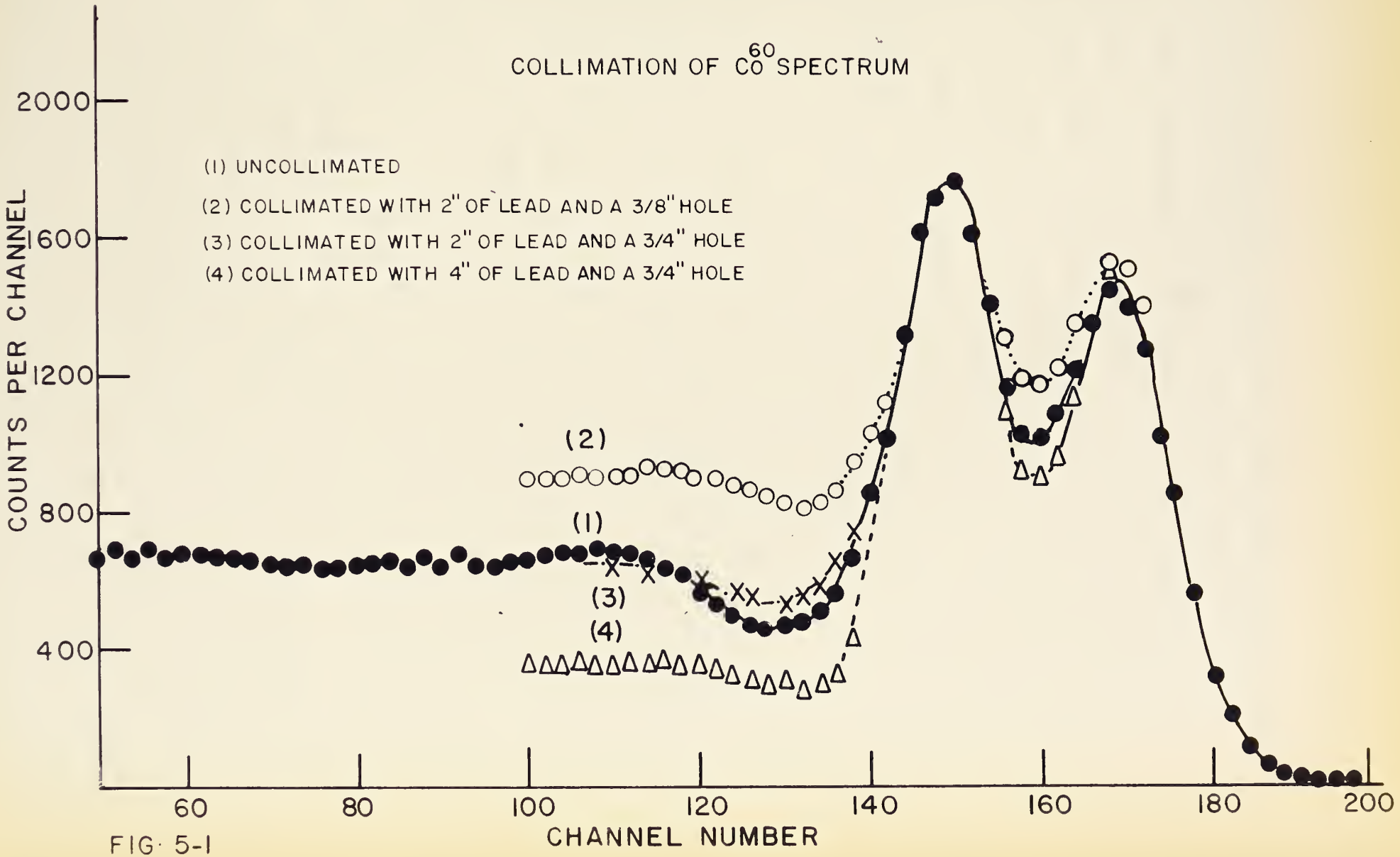
COLLIMATION OF Co^{60} SPECTRUM
(1) UNCOLLIMATED
(2) COLLIMATED WITH 2" OF LEAD AND A 3/8" HOLE
(3) COLLIMATED WITH 2" OF LEAD AND A 3/4" HOLE
(4) COLLIMATED WITH 4" OF LEAD AND A 3/4" HOLE
COUNTS PER CHANNEL
2000
1600
1200
800
400
(2)
(1)
(3)
(4)
60
80
100
120
140
160
180
200
CHANNEL NUMBER

FIG. 5-1

1.17 and 1.33 Mev photo peaks is considerably lower, thus increasing the resolution of the photo peaks.

The thickness of lead used for a collimator is important as it determines the fraction of the gamma rays which are transmitted through the lead. This fraction can easily be determined from the relation $\frac{N}{N_o} = e^{-\mu x}$, where x is the thickness of the lead and μ is the effective absorption coefficient for photons. A considerable fraction of the transmitted gammas are reduced in energy due to multiple scattering in lead. These multiple scattered gammas contribute to the "Compton", or degraded, spectrum. As the thickness of lead in the collimator increases, the intensity of the transmitted gammas is reduced, especially that of those which have reduced energy, lowering the "Compton" spectrum. Curve (3) and curve (4) illustrate the difference in the Compton level where 2" and 4" thick lead collimators are used to collimate the gamma rays of Co^{60} into a 4" NaI crystal. The spectrum (3), resulting when the 2" collimator is used, has a Compton level equivalent to that of the uncollimated spectrum.

The size of the collimation hole which determines the solid angle subtended by the crystal also affects drastically the area under the Compton spectrum. If the collimating hole is so small that the intensity of the

transmitted gamma rays is of the order of the intensity of the gamma rays incident on the crystal through the collimating hole, then the height of the Compton distribution is increased relative to the full energy peak. Curves (2) and (3) in Fig. 5-1 are spectra obtained using a 2" collimator with 3/8" diameter collimating hole and a 3/4" diameter collimating hole respectively. It is seen from Curve (2) that the Compton level has been increased considerably, to a higher level, in fact, than that of the uncollimated spectrum, and the resolution of the photo peak is reduced by filling in the valley between the photo peak and the Compton limit. The collimating geometry must suit the energy range of the gamma rays under investigation.

The collimator used for Hoogenboom studies is the 2" thick one with 3/4" diameter hole, which produces the spectrum shown by Curve (3) of Fig. 5-1. The second purpose of the collimator is just as important as effecting the increase in the photo peak efficiency. The 2" collimators used in the Hoogenboom spectrometer are equivalent to the 4" collimator for the single crystal. This is because the back scattered gamma rays must traverse 4 inches of lead before being detected in coincidence in the second crystal. Collimation, therefore, reduces the number of gate pulses which would be formed due to back scattering.

2. Efficiency

A comparison of the calcuated absolute efficiencies to the measured efficiencies for the collimated 4" NaI crystal is shown in the table in Section 3-2. The table is not very extensive since the efficiencies have been determined for the gamma rays from two sources only, Co^{60} and Na^{22}. With these limited results it is, however, possible to compare experimental and theoretical efficiencies. The table shows that there is reasonable agreement between the calculated values for the absolute efficiency of the collimated crystal and the experimentally determined photo peak efficiency. The experimental values of the photoefficiency are expected to be lower than the calculated values because the gamma rays transmitted through the lead collimator increase the height of the "Compton" spectrum, reducing the photo peak efficiency. To a good approximation the calculated values shown in Fig. 3-4 may, therefore, be used in calculating the Hoogenboom efficiency from expression 3-7 . It should be noted that the calculated values include the solid angle subtended by the collimator at the source. It is expected that a better agreement between the calculated efficiencies and experimental photo peak efficiencies would result if a 4" thick lead shield with 3/4" diameter collimating hole were used. This is evident from the

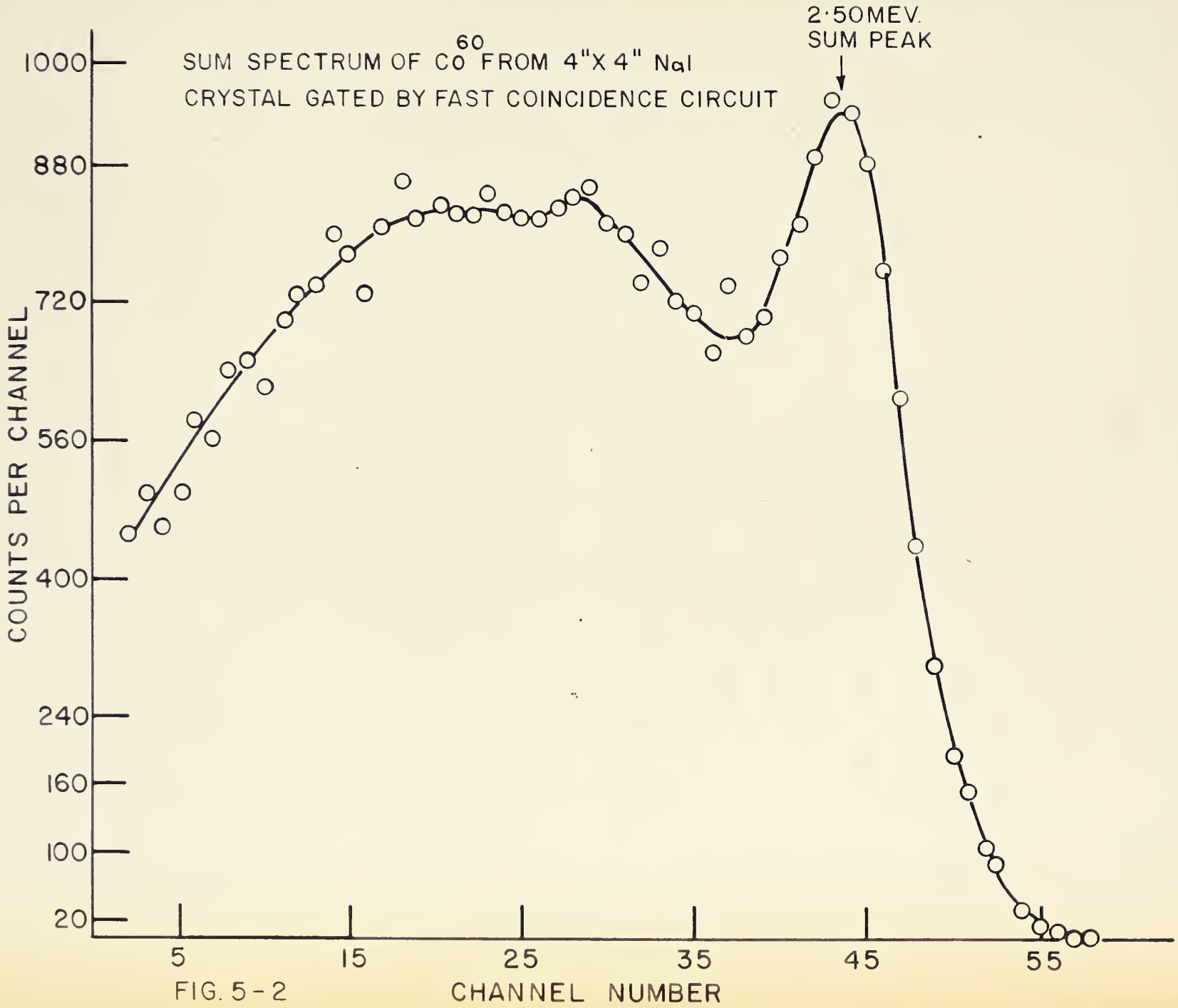
2·50MEV.
SUM PEAK
SUM SPECTRUM OF Co^{60} FROM 4"X 4" NaI
CRYSTAL GATED BY FAST COINCIDENCE CIRCUIT
1000
880
720
560
400
240
160
100
20
COUNTS PER CHANNEL
5
15
25
35
45
55
CHANNEL NUMBER

FIG. 5-2

comparison of curves (2) and (4) in Fig. 5-1 from which it is seen that the ratio R is larger for curve (4) than for curve (2).

That the experimental and the calculated values of the Hoogenboom efficiency are also in close agreement can be seen from the same table. The agreement is sufficiently close that the efficiency for detecting cascade gamma rays can be estimated by using the calculated absolute efficiency values for in the Hoogenboom efficiency expression. The Hoogenboom efficiency is very small and, therefore, the single crystal counting rates have to be rather high, of the order of 10^5 counts per second, to obtain a reasonable Hoogenboom counting rate.

3. Hoogenboom Spectra

A Hoogenboom spectrum consists of peaks corresponding to cascade gamma rays whose energies give the difference in energy levels of the nuclear state, between which the cascade appears. The sum pulse produced by the adding circuit is in coincidence with the pulse due to each of the cascade gamma rays. The sum peak should, therefore, be observed if the sum spectrum were gated to the kicksorter by the coincidence output of the fast coincidence circuit. Fig. 5-2 shows the sum spectrum of Co^{60} gated by the output of the fast coincidence circuit. Co^{60} emits gamma rays of 1.17 and 1.33 Mev in cascade and the sum peak

corresponds, therefore, to 2.5 Mev, as is shown in the Figure. It is also seen from the same curve that the sum spectrum contains a large "Compton" distribution as well as the sum peak. The large Compton spectrum may be attributed to the gamma rays scattered from one crystal into the other and to the gamma rays which have been transmitted through the collimator, as well as to escape of scattered quanta. Comparison of the magnitudes of the Compton distribution and photo peak in the sum spectrum with those in the single crystal spectrum shows that there is a large number of events in which a photon is scattered from one crystal to the other. It is possible to reduce this number greatly by using thicker collimators. 4" thick collimators rather than 2" collimators should be sufficient for the purpose.

The sum spectrum also indicates whether the energy calibration and the potentiometer setting of the adding circuit are correct. If one single crystal spectrum is not identical to the other, the sum spectrum tends to be flat without any evidence of a sum peak. It should be remembered, however, that the sum peak is resolved only if the single crystal photo peaks are resolved. The resolving time of the coincidence circuit should also be considered when the counting rate of each crystal is high, as the chance coincidence rate may become sufficiently high to contribute to the background level of the sum spectrum.

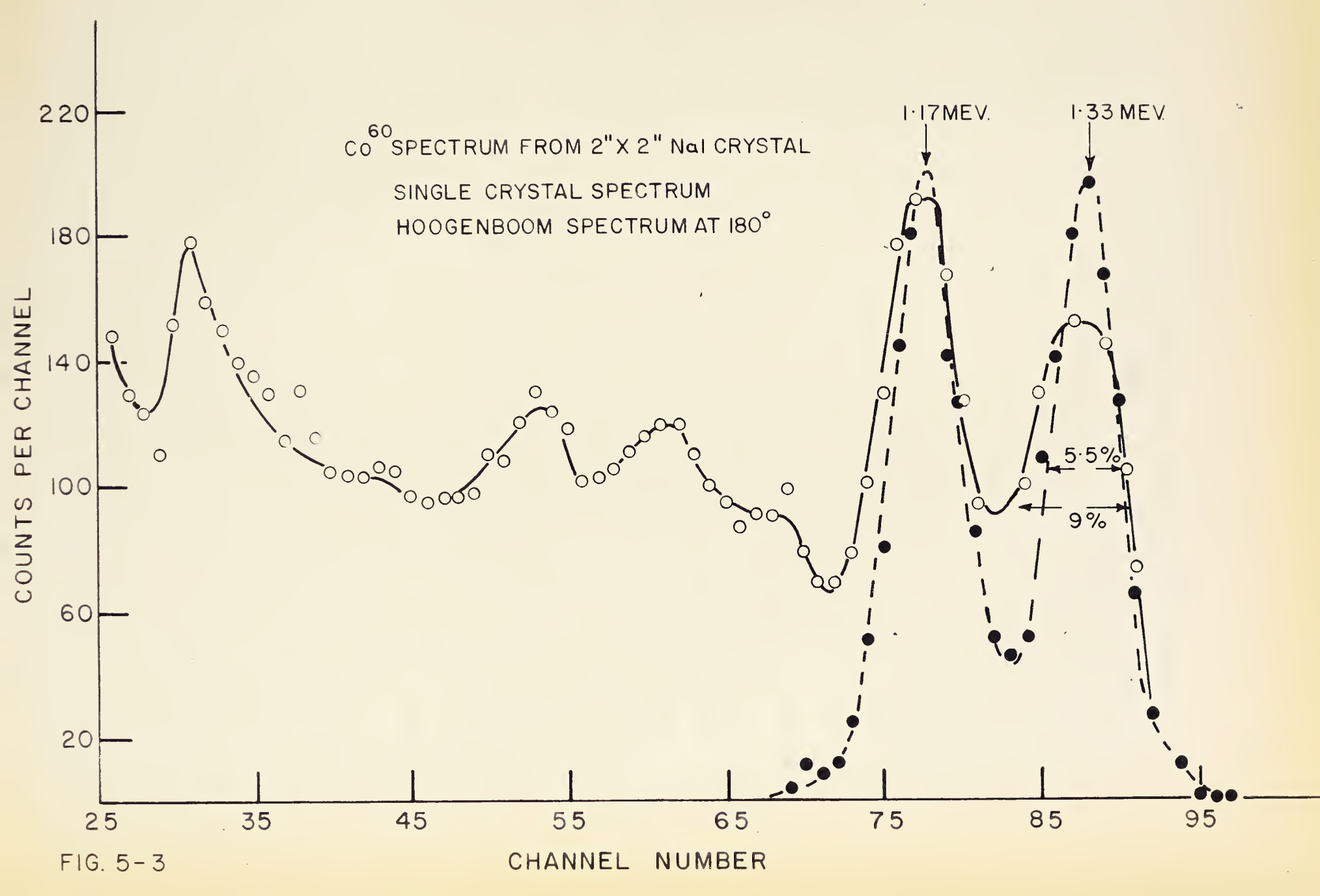
Co^{60} SPECTRUM FROM 2"X 2" NaI CRYSTAL
SINGLE CRYSTAL SPECTRUM
HOOGENBOOM SPECTRUM AT 180°
1·17MEV.
1·33 MEV.
5·5%
9%
COUNTS PER CHANNEL
CHANNEL NUMBER
220
180
140
100
60
20
25
35
45
55
65
75
85
95

FIG. 5-3

Co^{60} Spectrum

The Co^{60} is a β emitter, leaving Ni^{60} in its 2.505 Mev excited state which decays to the ground state by emitting 1.17 and 1.33 Mev gamma rays in cascade. The Co^{60} spectrum from a 2" crystal is shown in Fig. 5-3 and a 4" crystal in Fig. 5- 5 The spectra show the two photo peaks (1.17 Mev and 1.33 Mev) and some back scattered peaks superimposed on the Compton spectrum. The Compton level for a 2" crystal is expected to be higher than that of a 4" crystal because of the higher probability of escape of Compton scattered photons from a 2" crystal.

The total energy of the cascade in Co^{60} is 2.505 Mev. By setting the sum differential discriminator at a pulse height corresponding to 2.5 Mev with a window width of 2%, one obtains the Hoogenboom spectrum shown by the broken line in Fig. 5-3.

The Compton distribution has been completely eliminated from the Hoogenboom spectrum and the valley between the two photo peaks has been considerably lowered, thus improving the resolution. The sum peak does not appear because the fast coincidence circuit eliminates the possibility of displaying the case where both gamma rays strike one crystal and lose their energies completely to give the 2.5 Mev peak. The best resolution obtained is 5.5% at 1.33 Mev, the value obtained by Hoogenboom (Hoo).

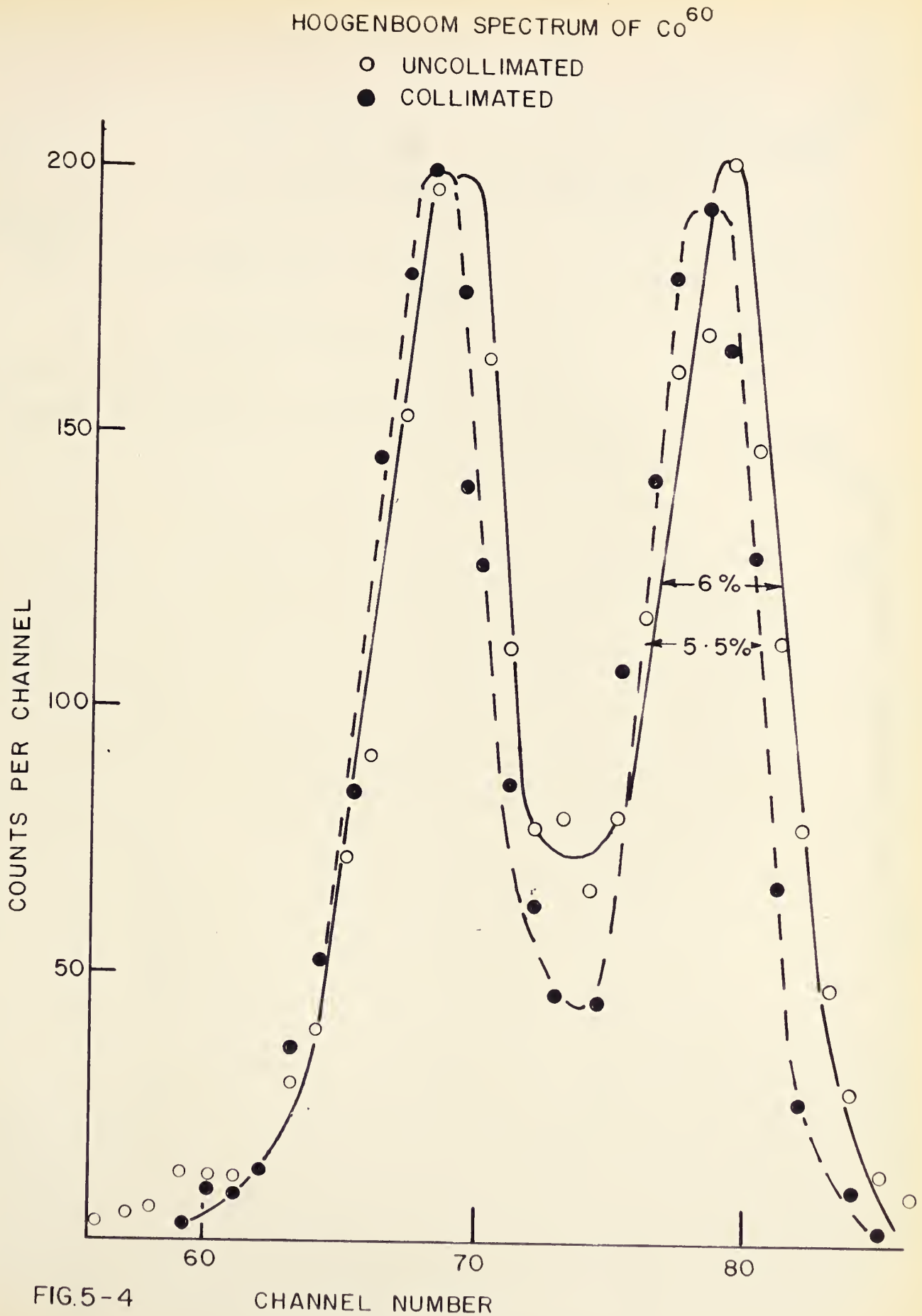
HOOGENBOOM SPECTRUM OF Co^{60}
UNCOLLIMATED
COLLIMATED
200
150
100
50
COUNTS PER CHANNEL
6 %
5·5%
60
70
80
CHANNEL NUMBER

FIG. 5-4

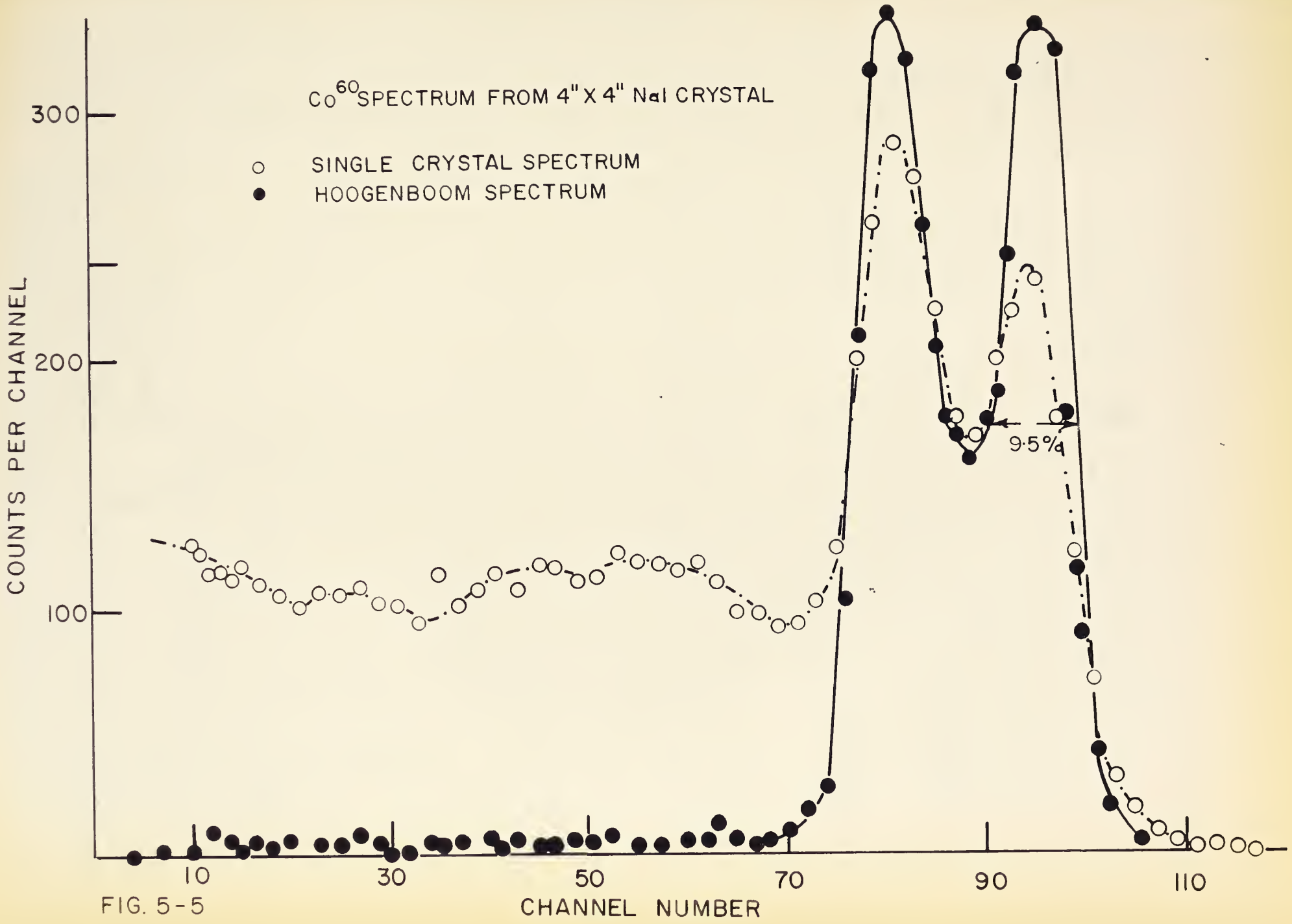
Co^{60} SPECTRUM FROM 4" X 4" NaI CRYSTAL
SINGLE CRYSTAL SPECTRUM
HOOGENBOOM SPECTRUM
9·5%
COUNTS PER CHANNEL
300
200
100
10
30
50
70
90
110
CHANNEL NUMBER

FIG. 5-5

HOOGENBOOM RESULTS FROM HOOGENBOOM, A.M. NUCLEAR INSTRUMENTS VOL. 3 (1958) 57

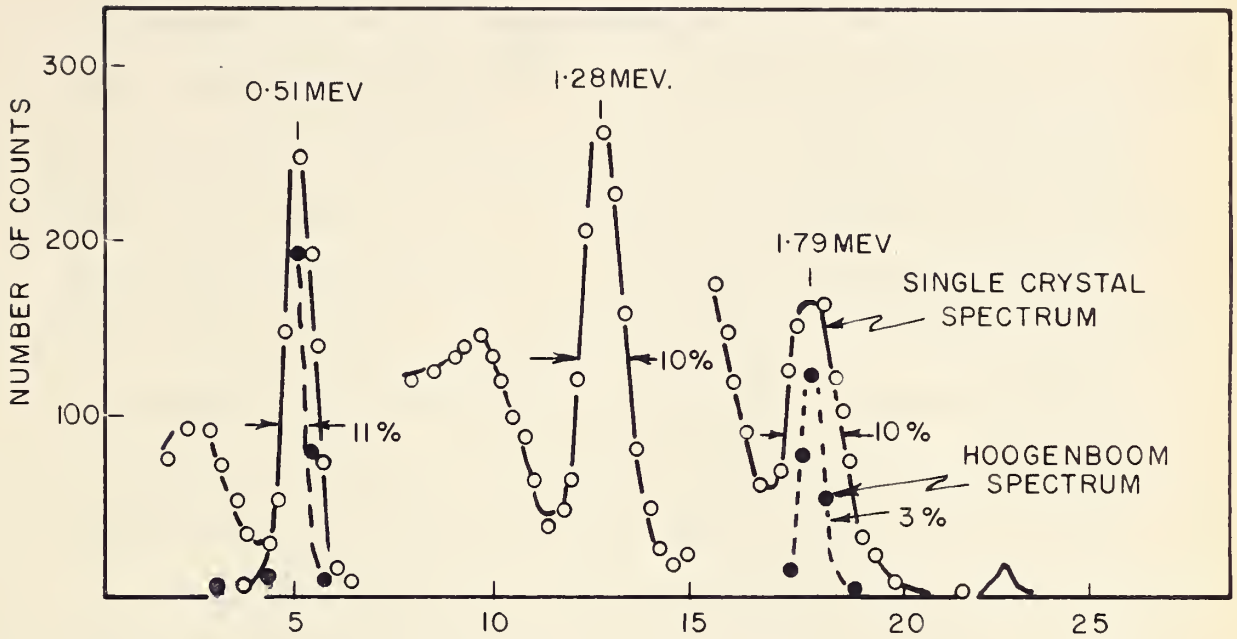

SINGLE CRYSTAL AND HOOGENBOOM SPECTRUM USING 2" NaI CRYSTAL AT 180 AND SUM CHANNEL AT 2·2 MEV.

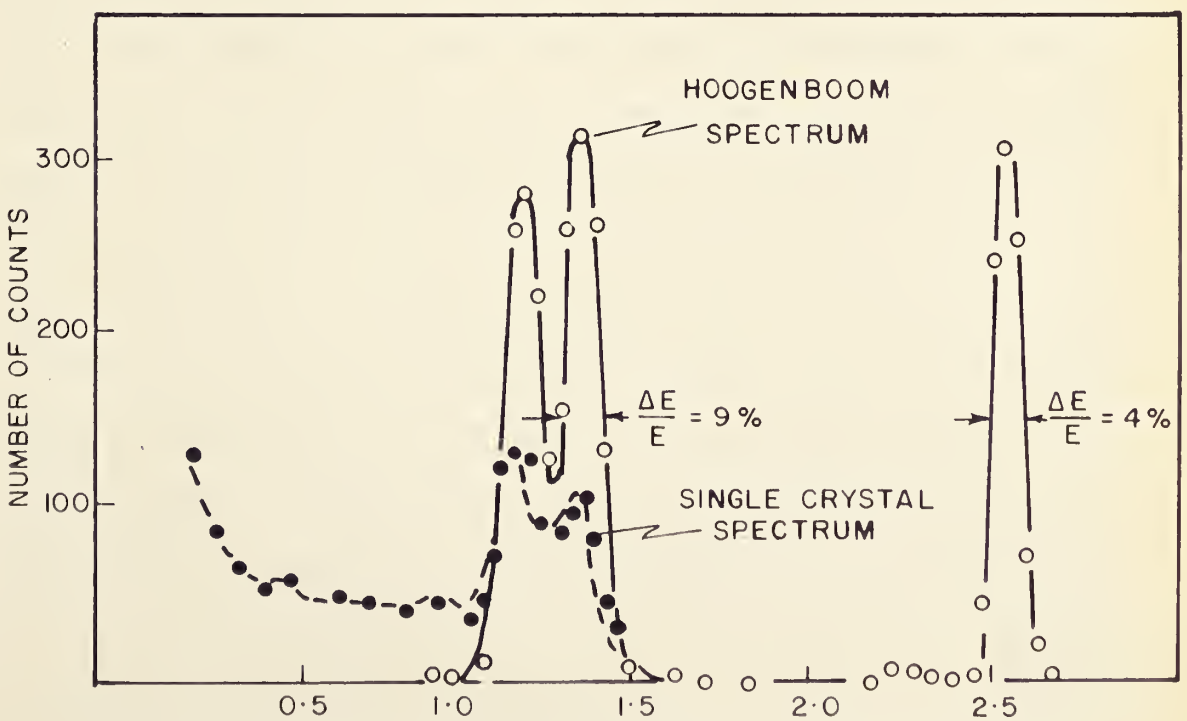

FIG. 5-6 SINGLE CRYSTAL AND HOOGENBOOM SPECTRUM USING 4" NaI CRYSTAL AT 180 AND SUM CHANNEL AT 2·5 MEV.

This spectrum verifies the theoretical predictions of Chapter III of 6% resolution at 1.33 Mev. The photo peaks have equal full widths at half maximum, $\Gamma_{s_1} = \Gamma_{s_2} = 73$ kev as compared to the calculated value, 80 Kev. The areas under the peaks are equal within statistical error, verifying that the efficiencies for detecting the cascade gamma rays are equal, that is $\varepsilon_{s_1} \simeq \varepsilon_{s_2}$. Collimation of the gamma rays is effective in improving the resolution of the spectrometer. Fig. 5-4 shows that the collimated spectrum has an improvement of about 0.5% in resolution.

The Co^{60} spectrum from the 4" x 4" NaI crystals is shown by the broken line in Fig. 5-5 and the corresponding Hoogenboom spectrum is shown by the solid line. The resolution for the Hoogenboom spectrum, using 5% window width at 2.5 Mev, is 9.5%. This value of resolution differs from that obtained by Hoogenboom by 0.5%. The single crystal spectrum published by Hoogenboom (Fig. 5-6) shows poorer photo peak resolution than that obtained here. Therefore, the gated Hoogenboom spectrum should have a resolution better than that obtained by Hoogenboom (Fig. 5-6). When the width of the differential discriminator window is reduced to 4% or lower, the gated spectrum appears to be chopped and the valley between the two photo peaks begins to fill in, resulting in a decrease in resolution. This decrease in resolution may

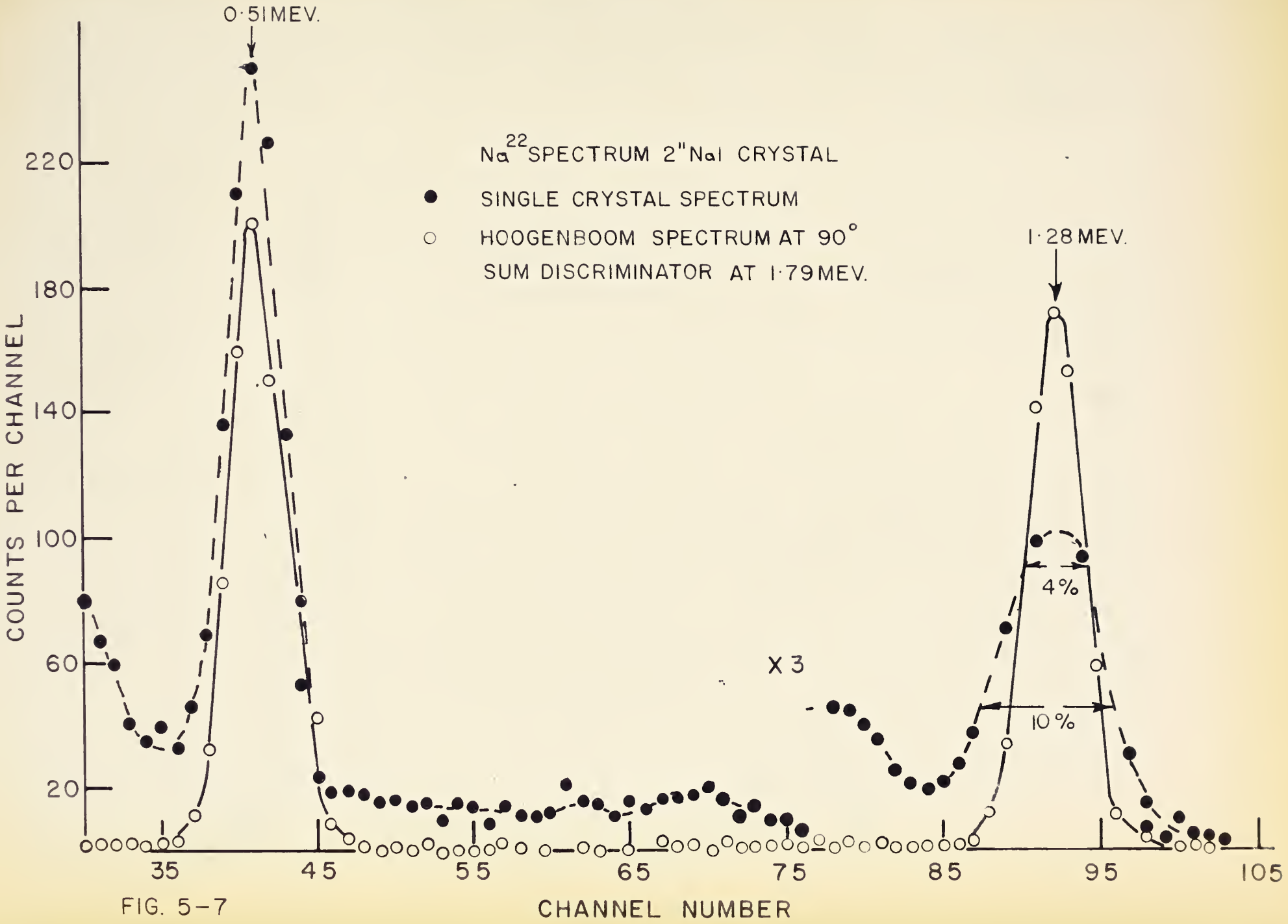
0·51MEV.
Na22 SPECTRUM 2"NaI CRYSTAL
SINGLE CRYSTAL SPECTRUM
HOOGENBOOM SPECTRUM AT 90°
SUM DISCRIMINATOR AT 1·79MEV.
1·28MEV.
4%
10%
X3
COUNTS PER CHANNEL
CHANNEL NUMBER
220
180
140
100
60
20
35
45
55
65
75
85
95
105

FIG. 5–7

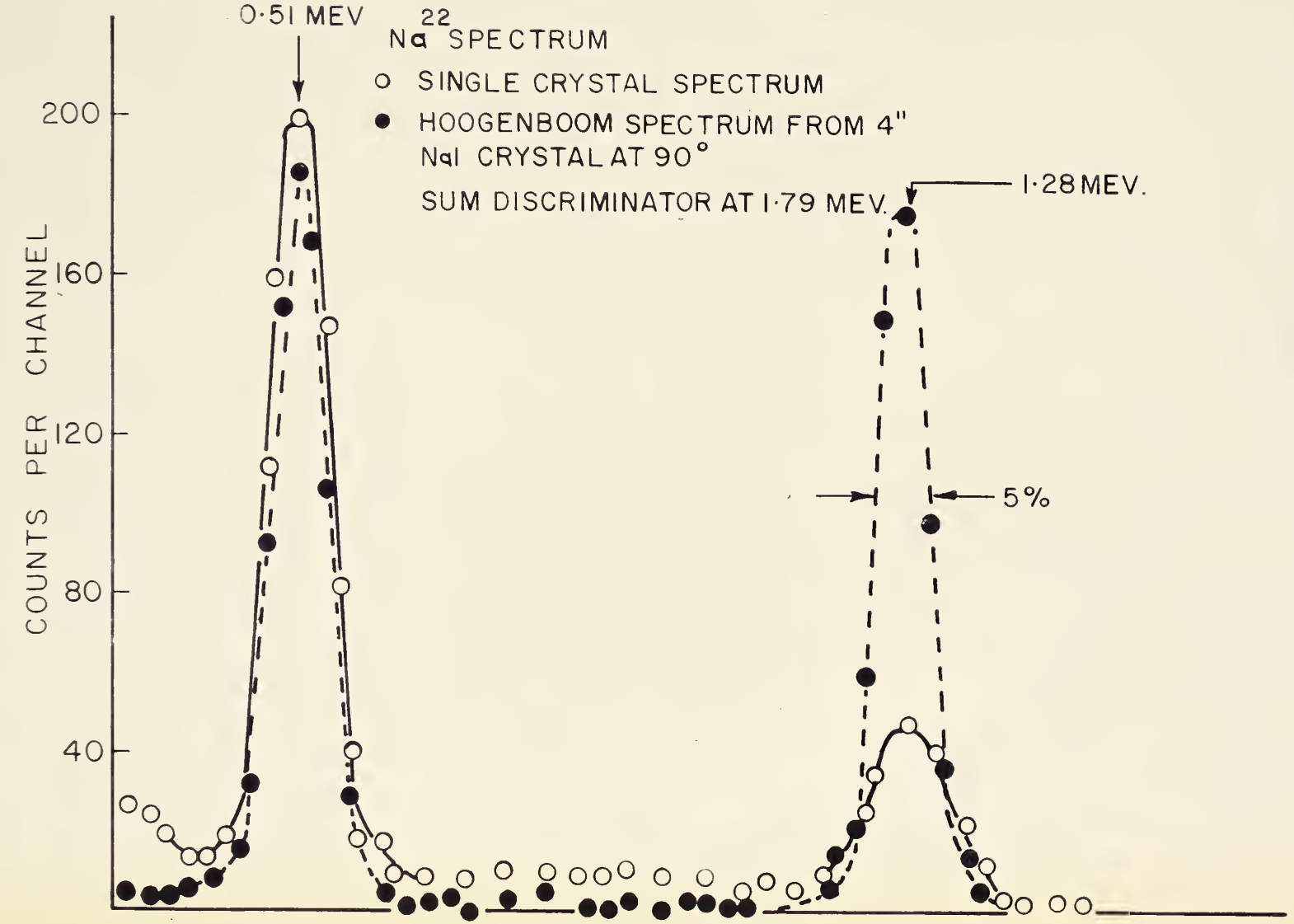
0·51 MEV
Na^{22} SPECTRUM
SINGLE CRYSTAL SPECTRUM
HOOGENBOOM SPECTRUM FROM 4" NaI CRYSTAL AT 90°
SUM DISCRIMINATOR AT 1·79 MEV.
1·28 MEV.
5%
COUNTS PER CHANNEL
200
160
120
80
40
40
60
80
100
120
140
160
CHANNEL NUMBER

FIG. 5-8

result from the fact that resolving time of the fast coincidence circuit is not sufficient to reduce the number of chance coincidences, which is of the order of the number of true gating pulses. When counting rates are decreased by a factor of 10, the Hoogenboom counting rate is decreased by a factor of 100; hence it is necessary to take long runs during which electronic gain drifts may occur, resulting in poor resolution. Fig. 5-5 shows the Hoogenboom spectrum for a single crystal counting rate of 1.5×10^4 counts per second, giving 9.5% resolution at 1.33 Mev.

Na^{22} Spectrum

A Na^{22} nucleus may emit a positron leaving Ne^{22} in the 1.28 Mev state, which decays by gamma emission to the ground state. The Na^{22} spectrum, therefore, consists of the 0.51 Mev annihilation photo peak and the 1.28 Mev photo peak. The 2" NaI crystal spectrum of Na^{22} is shown in Fig. 5-7 and the 4" NaI crystal spectrum is shown in Fig. 5-8.

The annihilation of a positron usually causes creation of two 0.51 Mev gamma rays travelling in opposite directions. The Hoogenboom spectrum, therefore, is different when the counters are set at 180° from that when the counters are set at 90°. At 180° the possible sum peaks are at 1.02 Mev and 2.30 Mev, and at 90° the only possible sum peak is at 1.79 Mev. When the counters

are set at 180° and are symmetrical in solid angle there is no possibility of having a 1.79 Mev sum peak because for each annihilation gamma ray detected in one crystal, the second annihilation gamma ray from annihilation of the same positron is detected in the second crystal resulting always in 1.02 Mev sum. When the 1.28 Mev gamma ray is incident on one crystal in coincidence with a 0.51 Mev in the other then the added sum will be 2.3 Mev because of the second annihilation gamma ray. Setting the sum differential discriminator at 2.3 Mev will, therefore, result in only the 0.51 Mev and 1.79 Mev (0.51 Mev plus 1.28 Mev) photo peaks. The 1.28 Mev photo peak is not observed. If, however, the source is not centered properly, or if considerable scattering occurs between the two crystals, there is a possibility that the 1.28 Mev gamma ray peak may be displayed in the Hoogenboom spectrum. It, however, is expected to be considerably smaller in height than the height of the 0.51 Mev and 1.79 Mev peaks.

At 90° the only possible sum peak is at 1.79 Mev. With the sum differential discriminator set at this value the only photo peaks which appear in the Hoogenboom spectrum are 0.51 Mev and 1.28 Mev. Fig. 5-7 shows the single crystal and the Hoogenboom spectrum resulting from 2" NaI crystals at 90° separation. The Hoogenboom spectrum is free of the Compton distribution which is present in the single crystal spectrum. The resolution

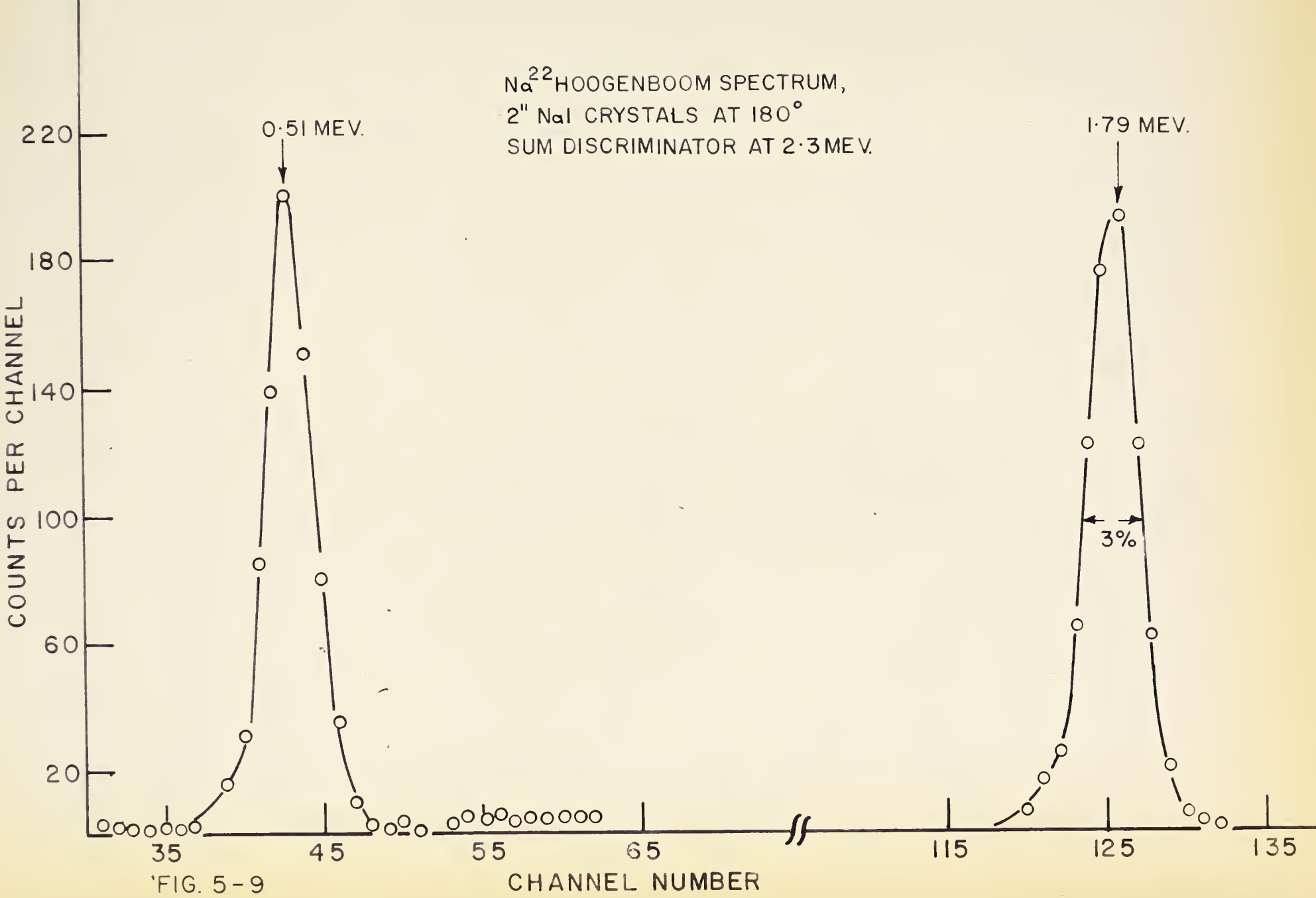
Na22 HOOGENBOOM SPECTRUM,
2" NaI CRYSTALS AT 180°
SUM DISCRIMINATOR AT 2·3 MEV.
0·51 MEV.
1·79 MEV.
3%
220
180
140
100
60
20
COUNTS PER CHANNEL
35
45
55
65
115
125
135
CHANNEL NUMBER

FIG. 5-9

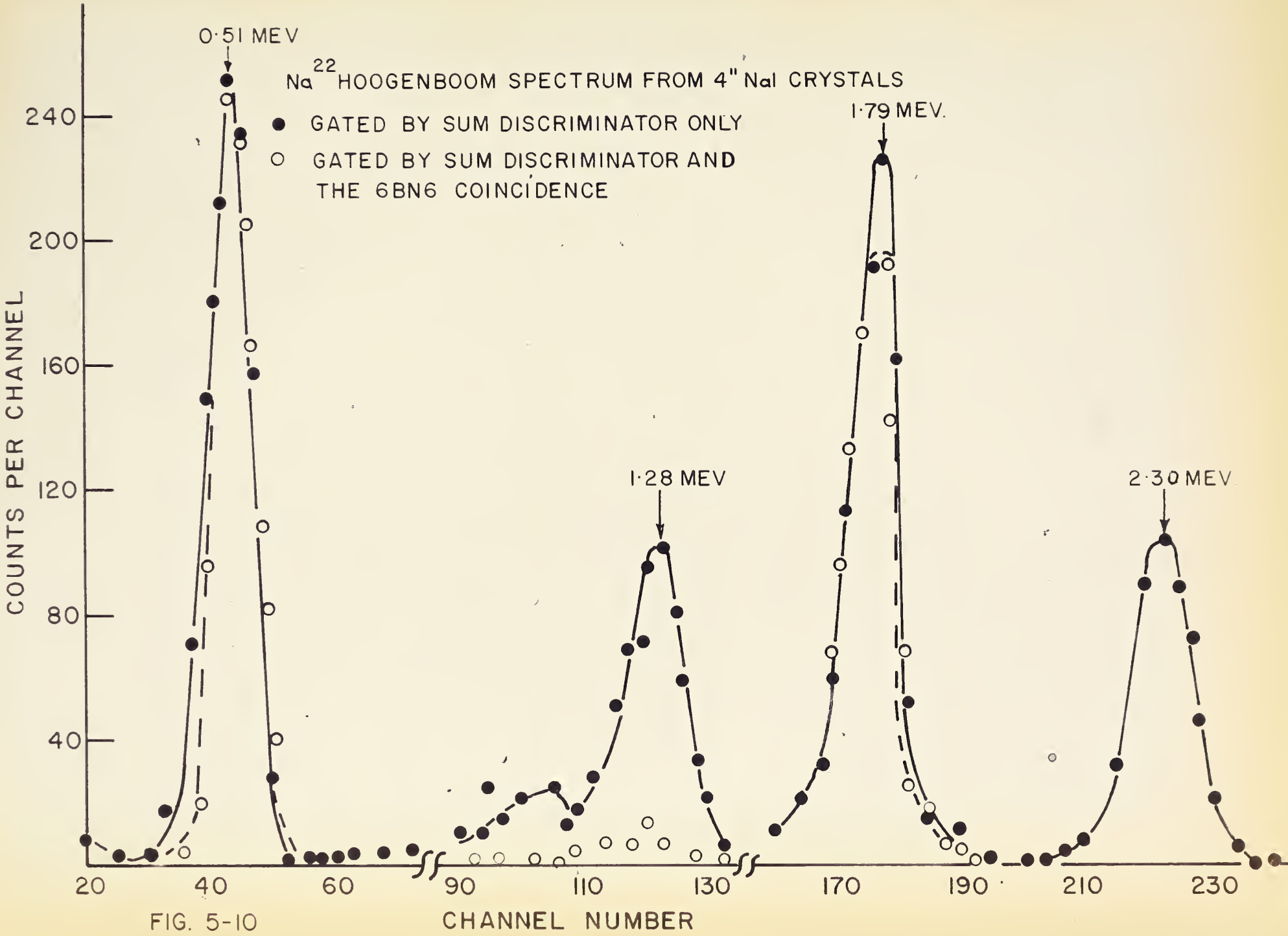
0·51 MEV
Na 22 HOOGENBOOM SPECTRUM FROM 4" NaI CRYSTALS
GATED BY SUM DISCRIMINATOR ONLY
GATED BY SUM DISCRIMINATOR AND THE 6BN6 COINCIDENCE
1·79 MEV.
1·28 MEV
2·30 MEV
COUNTS PER CHANNEL
240
200
160
120
80
40
20
40
60
90
110
130
170
190
210
230
CHANNEL NUMBER

FIG. 5-10

of the photo peak is greatly improved. In particular, the 1.28 Mev photo peak has the resolution improved from 10% to 4% with the window of the sum discriminator set at 2%. This is smaller than the theoretically predicted value of 5% at 1.28 Mev and is in agreement with the Hoogenboom results. The measured Hoogenboom widths at half maximum are found to be $\Gamma_{S1} = 53$ Kev and $\Gamma_{S2} = 51$ Kev, respectively, which are nearly equal. The area under the photo peaks is approximately the same, so the Hoogenboom efficiency ε_{1S} and ε_{2S} of the two cascading gamma rays γ_1 and γ_2 is the same.

When the two detectors are separated by 180° with the sum discriminator set at 2.3 Mev, the resultant Hoogenboom spectrum from the 2" NaI crystal is shown in Fig. 5-9. To obtain this spectrum the counters must be equidistant from the source, as checked by directly measuring the source distance from each counter and by comparing the counting rates of the detectors. The two methods agree within statistical error. The Hoogenboom spectrum then shows only the two peaks expected, at 0.51 Mev and 1.79 Mev, there being no evidence of a 1.28 Mev photo peak. The 1.79 Mev peak has a width of 3%, when the sum discriminator is set at 2%, in agreement with Hoogenboom. When the window setting is increased to 5% at 2.3 Mev, thus allowing some back scattered gamma

rays to operate the gate, the 1.28 Mev peak begins to appear above the background level of the spectrum.

Fig. 5-10 shows two Hoogenboom spectra from 4" NaI crystals placed 180° apart. One is gated by the sum discriminator only and the other is gated by the sum discriminator together with the fast coincidence circuit. There is considerable difference between the two spectra. The spectrum gated by the sum discriminator alone shows both of the single gamma photo peaks, which are the 0.51 Mev and the 1.28 Mev peaks, together with the sum peaks at 1.79 Mev and 2.30 Mev. These sum peaks correspond to the possible combinations of the single gamma energies. The second spectrum shows only the 0.51 Mev and the 1.79 Mev peaks which, when added together, give 2.3 Mev, the value on which the sum discriminator is set. Both spectra are obtained when the sum discriminator window width is 4%. The counting rate of crystal 2 was greater by 5% than that of crystal 1. The high counting rate of crystal 1, 10^4 per second, and the rather long effective resolving time, 1 μ sec., of the sum gate, combine to produce sufficient chance sum pulses to gate the 1.28 gamma onto the display. By inserting the fast coincidence circuit these chance sum pulses are eliminated as is shown by the second spectrum. The difference in widths of the peaks is small; the improvement favours fast coincidence gating.

When the window width of the sum discriminator is

decreased to 3%, the resulting spectrum is shown in Fig. 5-11. The 1.79 Mev sum peak width is 4%. Fig. 5-12 illustrates the Na^{22} Hoogenboom spectrum when the 4" counters are placed at 90° and the window of the sum discriminator, is set at 3.5%, giving 5% resolution at 1.28 Mev.

For a nucleus having more complex decay scheme than those considered here, the Hoogenboom spectrum has peaks corresponding to all the possible combinations of the gamma energies which, when added together, form the sum energy corresponding to the sum discriminator setting. The peaks of the gated spectrum have approximately constant widths provided the width of the sum discriminator is set to ensure that $\Gamma_1 \gg \Gamma_s$ where Γ_1 is the width of the narrowest photo peaks in the single crystal spectrum and Γ_s is the width of the sum discriminator window. The areas under the peaks in the gated spectrum are in the ratio of the intensities of the cascade gamma rays from the sum level, provided that the counting rates of the two detectors are equal.

The Hoogenboom spectrometer is a useful device for determining the energy of cascade gamma rays from an excited nucleus, provided sufficiently high intensities are available. Counting rates of 10×10^3 counts/sec. are necessary to obtain meaningful data within a reasonable length of time.

Though this is a serious limitation, the spectrometer may be used in many cases to measure the angular correlations of cascade gamma rays. This data is often sufficient to assign, or at least restrict, the values of the angular momenta of the nuclear states involved. In addition to these applications to nuclear spectroscopy, there is a more interesting potentiality, that of measuring the probabilities of gamma ray transitions. Such measurements provide a sensitive check of theoretical predictions based on the intermediate coupling shell model.

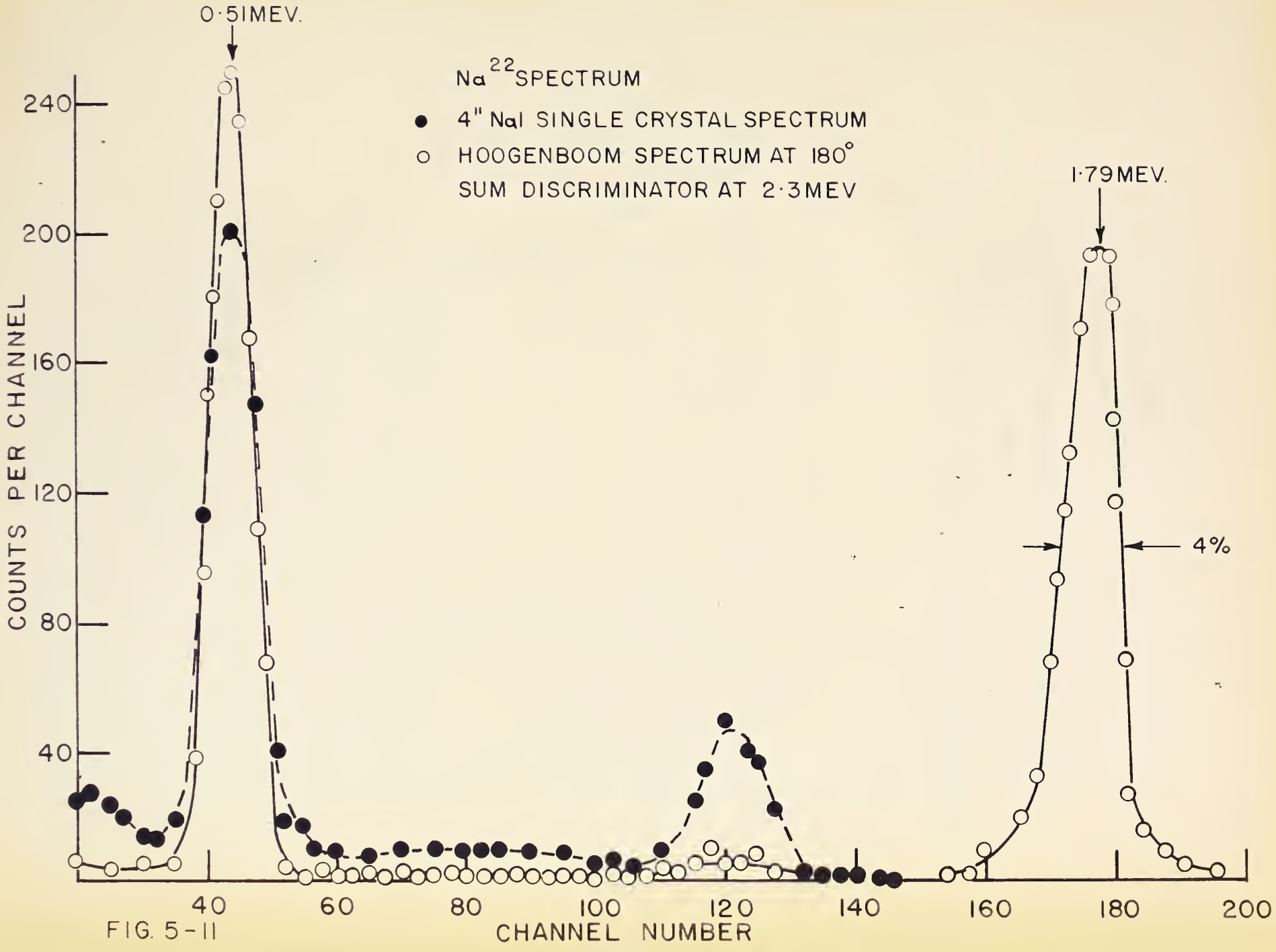
0·51MEV.
Na 22 SPECTRUM
4" NaI SINGLE CRYSTAL SPECTRUM
HOOGENBOOM SPECTRUM AT 180°
SUM DISCRIMINATOR AT 2·3MEV
1·79MEV.
4%
COUNTS PER CHANNEL
240
200
160
120
80
40
40
60
80
100
120
140
160
180
200
CHANNEL NUMBER

FIG. 5-11

APPENDIX

The total linear absorption cross section μ cm^{-1} for NaI is given in the table below. The values of μ are obtained from Siegbahn, Beta and Gamma Ray Spectroscopy, Ch. V, Sect. 5.

E Mev	$\mu(E)$ cm^{-1} ± 0.002
0.50	0.330
1.17	0.242
1.33	0.180
1.50	0.170
2.10	0.148
2.60	0.138
3.00	0.134
4.00	0.129
5.00	0.127
7.50	0.130
10.00	0.138

BIBLIOGRAPHY

(Al) R. D. Albert. Rev. Sci. Instr. 24 (1953) 1096.

(He) W. Heitler. The Quantum Theory of Radiation, 2nd. Ed. Oxford Univ. Press, Ch. III.

(Hea) R. L. Heath. Scintillation Spectrometry, Gamma-Ray Spectrum Catalogue. Phillips Pet. Atomic Energy Div. (IDO-16408) (1957).

(Ho) R. Hofstadter and J. A. McIntyre. Phys. Rev. 78 (1950) 619.

(Hoo) A. M. Hoogenboom. Nuclear Instr. 3 (1958) 57.

(Jo) P. J. Riley. M.Sc. Thesis, U.B.C. (1957).

(Ka) H. Kallman and M. Furst. 78 (1950) 621.

(Ma) F. C. Maienschein and J. K. Blair. Phys. Rev. 28 (1951) 317A.

(Mo) W. E. Mott and R. B. Sutton. Handbuch der Physik. Vol. XLV, Sect. 8, 9.

(Ri) Richtmyer, Kennard and Lauritsen. Introduction to Modern Physics, 5th Ed. McGraw Hill, Ch. 8, Sect. 160.

(Sa) J. T. Sample, G.C. Neilson, G. Chadwick, J.B. Warren. Can. J. Phys. 33 (1955) 828.

(Se) E. Segre. Experimental Nuclear Physics. Wiley and Sons, Vol. I, Pt.II, Sect. 3.

(Si) S. Siegbahn. Beta and Gamma-Ray Spectroscopy. North Holland, Ch. V, Sect. 7.

(Si a) _____. Sect. 5.

(Si b) _____. Ch. VII, Sect. 9.

(Si c) _____. Ch. V, Sect. 3.